ARCHIVIO ISTITUZIONALE
DELLA RICERCA

Alma Mater Studiorum Università di Bologna
Archivio istituzionale della ricerca

Reversal of neurodevelopmental impairment and cognitive enhancement by pharmacological intervention with the polyphenol polydatin in a Down syndrome model

This is the final peer-reviewed author's accepted manuscript (postprint) of the following publication:

Published Version:
Emili, M., Stagni, F., Russo, C., Angelozzi, L., Guidi, S., Bartesaghi, R. (2024). Reversal of neurodevelopmental impairment and cognitive enhancement by pharmacological intervention with the polyphenol polydatin in a Down syndrome model. NEUROPHARMACOLOGY, 261, 1-18 [10.1016/j.neuropharm.2024.110170].

Availability:
This version is available at: https://hdl.handle.net/11585/990497 since: 2025-06-25

Published:

DOI: http://doi.org/10.1016/j.neuropharm.2024.110170

Terms of use:

Some rights reserved. The terms and conditions for the reuse of this version of the manuscript are specified in the publishing policy. For all terms of use and more information see the publisher's website.

This item was downloaded from IRIS Università di Bologna (https://cris.unibo.it/).
When citing, please refer to the published version.

(Article begins on next page)

06 November 2026

Title: Reversal of neurodevelopmental impairment and cognitive enhancement by pharmacological intervention with the polyphenol polydatin in a Down syndrome model

Authors

Marco Emili [a], Fiorenza Stagni [a], Carla Russo [a], Laura Angelozzi [a], Sandra Guidi [b], Renata Bartesaghi [b] *

a Department for Life Quality Studies, University of Bologna, Rimini, Italy

b Department of Biomedical and Neuromotor Sciences, University of Bologna, Bologna, Italy

* Corresponding author:
Prof. Renata Bartesaghi
Department of Biomedical and Neuromotor Sciences
Physiology Building
Piazza di Porta San Donato 2
I-40126 BOLOGNA BO, Italy
Tel +39 051 2091727
E-mail renata.bartesaghi@unibo.it

ABSTRACT

Intellectual disability (ID) is the unavoidable hallmark of Down syndrome (DS), a genetic condition due to triplication of chromosome 21. ID in DS is largely attributable to neurogenesis and dendritogenesis alterations taking place in the prenatal/neonatal period, the most critical time window for brain development. There are currently no treatments for ID in DS. Considering the timeline of brain development, treatment aimed at improving the neurological phenotypes of DS should be initiated as early as possible and use safe agents. The goal of this study was to establish whether it is possible to improve DS-linked neurodevelopmental defects through early treatment with polydatin, a natural polyphenol. We used the Ts65Dn mouse model of DS and focused on the hippocampus, a brain region fundamental for long-term memory. We found that in Ts65Dn mice of both sexes treated with polydatin from postnatal (P) day 3 to P15 there was full restoration of neurogenesis, neuron number, and dendritic development. These effects were accompanied by normalization of cyclin D1 and DSCAM levels, which may account for the rescue of neurogenesis and dendritogenesis, respectively. Importantly, in Ts65Dn mice treated with polydatin from P3 to adolescence (~P50) there was full restoration of hippocampus-dependent memory, indicating a pro-cognitive outcome of treatment. No adverse effects were observed on the body and brain weight. The efficacy and safety of polydatin in a model of DS prospect the possibility of its use during early life stages for amelioration of DS-linked neurodevelopmental alterations.

Key words: Down syndrome; Intellectual disability; Neurodevelopmental alterations; Neonatal therapy; Officinal drugs; Polyphenols

1. INTRODUCTION

Down syndrome (DS) is a relatively high incidence pathology (1:750-1000) (de Graaf et al., 2021) caused by triplication of chromosome 21 (Chr21) (reviewed by (Bull, 2020)). A particularly severe consequence of trisomy 21 is impairment of the neurological development starting from fetal life stages, with ensuing intellectual disability (reviewed by (Bartesaghi et al., 2011; Delabar et al., 2006; Dierssen, 2012; Haydar and Reeves, 2012)). The major neurodevelopmental alterations in DS consist in a reduction of neurogenesis (see (Stagni et al., 2018)). and impairment of dendritic morphogenesis, with generalized dendritic hypotrophy and reduction of dendritic spine density (Benavides-Piccione et al., 2004; Ferrer and Gullotta, 1990; Marin-Padilla, 1976; Purpura, 1975; Takashima et al., 1981; Takashima et al., 1994). These defects are thought to be largely responsible for the intellectual disability that characterizes DS. Intense efforts have been made during the past twenty years to establish whether it is possible to pharmacologically improve these alterations. Indeed, preclinical studies in DS mouse models have identified various drugs that improve or even restore brain development and cognitive performance (reviewed by (Bartesaghi et al., 2011; Costa and Scott-McKean, 2013; Gardiner, 2015; Rueda et al., 2020; Stagni and Bartesaghi, 2022; Stagni et al., 2015a)). Demonstration that DS-linked brain alterations may be pharmacologically ameliorated in DS models gives a glimpse of hope. Yet, caveats due to potential side effects of some of the tested drugs may hinder or prevent their use in individuals with DS. This problem could be overcome by identification of new substances that similarly to drugs restore brain development but that, due to their nature, may warrant a safer profile.

Plant-derived natural substances have been traditionally used by mankind to overcome a gamut of illnesses. Currently a series of substances, including polyphenols, are attracting the attention as a possible means to ameliorate neurodevelopmental disorders because they change the expression of genes and the activity of pathways involved in brain development (see (An et al., 2022)). Among polyphenols, resveratrol has aroused great interest during the past twenty years due to its many healing effects (Zhang et al., 2021). Regarding the brain, research has shown that resveratrol positively impacts various psychiatric disorders (Shayganfard, 2020), enhances hippocampal neurogenesis (Kumar et al., 2016), increases dendritic length and dendritic spine density (Monserrat Hernandez-Hernandez et al., 2016), and protects against neurodegeneration in models of Alzheimer's disease (Kim

et al., 2007). It has been additionally shown that resveratrol improves neurogenesis and mitochondrial function in neural progenitor cells derived from Ts65Dn mice (Valenti et al., 2016), suggesting that this polyphenol may represent a suitable treatment for DS. It must be noted, however, that despite its widespread benefits, the low bioavailability of resveratrol may represent a critical obstacle to clinical application (Walle et al., 2004).

Polydatin (Poly) is a glucoside of resveratrol that was originally isolated from Polygonum cuspidatum and is also contained in grape, peanut, and red wines. It is a traditional Chinese medicine that has long been used in China as an analgesic, anti-pyretic, and diuretic (Du et al., 2013). Unlike resveratrol, Poly is absorbed by active transport systems in the gastrointestinal apparatus where it is deglycosylated in trans-resveratrol (Du et al., 2013). Since it is practically completely absorbed by the intestinal apparatus, it can be effective at doses lower than those of resveratrol. Moreover, Poly is more resistant than resveratrol to enzymatic oxidation and can penetrate the cell through an active transport mechanism (Du et al., 2013). A pharmacokinetic study indicated that Poly crosses the blood-brain barrier (Lv et al., 2006). Numerous investigations report physiological benefits of Poly on the heart (Zhang et al., 2017), liver (Tang et al., 2022), lung (Tang et al., 2019), metabolic diseases (Luo et al., 2022) (see also (Du et al., 2013; Karami et al., 2022)) and even as an agent that may counteract the complications of COVID-19 (Ricordi et al., 2021). Regarding the brain, it appears that Poly has neuroprotective activity in lipopolysaccharide-Induced Parkinson's Disease (Huang et al., 2018), cerebral ischemic damage and chronic alcoholism and, since it inhibits amyloid-β peptide aggregation, it may also exert some benefit in Alzheimer's disease (Du et al., 2013). Poly has been shown to possess a good drug-likeness and an *in silico* evaluation of its medicinal property has found numerous main targets, highlighting its pharmacological influences (Pan et al., 2018). If, as it seems reasonable, Poly exerts similar benefits on the brain as resveratrol, Poly may be used as treatment for brain dysfunctions, with the advantage that lower doses may be sufficient because of its higher bioavailability.

Based on all these premises, we wondered whether Poly may be a useful treatment for amelioration of brain development in DS. To obtain an answer to this question, we have used the Ts65Dn mouse, a DS model that has been used by most preclinical studies (reviewed by (Bartesaghi et al., 2011; Costa and Scott-McKean, 2013; Gardiner, 2015; Stagni and Bartesaghi, 2022; Stagni et al., 2015a)). We have treated mice in the early postnatal period based on the following rationale. The bulk of neurogenesis takes place prenatally (Kostović et al., 2019;

Rakic, 2009; Rice and Barone, 2010; Stiles and Jernigan, 2010; Yamaguchi et al., 2016). Hippocampal neurogenesis, however, mainly occurs in the neonatal period in rodents and continues at a slow rate throughout life in rodents as well as humans (Altman and Bayer, 1975; Altman and Bayer, 1990a; b; Spalding et al., 2013; Workman et al., 2013). Thus, although the prenatal period represents an ideal window of opportunity to improve neurogenesis in DS, the neonatal period can be exploited to foster hippocampal neurogenesis. Unlike neurogenesis, dendritic development and maturation largely take place in the early postnatal period in both rodents and humans (Becker et al., 1984; Koester and O'Leary, 1992; Lu et al., 2013). Therefore, the neonatal period of rodents provides the unique opportunity to explore the effects of a given drug on two key developmental processes that are altered in DS, i.e. neurogenesis and dendritogenesis. We show here that early treatment with Poly restores neurogenesis, cellularity, dendritic maturation, and cognitive performance in Ts65Dn mice, with no patent adverse effects. Thus, this natural compound may represent an attractive possibility in the field of treatments for amelioration of intellectual disability in individuals with DS.

2. METHODS

2.1. Colony

Ts65Dn mice were generated by mating B6EiC3Sn a/A-Ts(17^16)65Dn females (1924 line) with C57BL/6JEiJ x C3H/HeSnJ (B6EiC3Sn) F1 hybrid males. This parental generation was provided by Jackson Laboratories (Bar Harbor, ME, USA). New Ts65Dn females, obtained from the Jackson Laboratory every ~6 months, were introduced into the breeding colony to maintain a constant generation of animals, and correct for possible genetic drift. To maintain the original genetic background, we used for treatment mice of the first generation of this breeding. Animals were genotyped as previously described (Reinholdt et al., 2011). The day of birth was designated as postnatal day zero (P0). The animals' health and comfort were controlled by the veterinary service. The animals had access to water and food *ad libitum* and lived in a room with a 12:12 h light/dark cycle. Experiments were performed in accordance with the European Communities Council Directive of 24 November 1986 (86/609/EEC) for the use of experimental animals and were approved by Italian Ministry of Public Health

(558/2023-PR). All efforts were made to minimize animal suffering and to keep the number of animals used to a minimum.

2.2. Experimental plan

The overall purpose of our study was to establish whether early treatment with Poly improves DS-linked impairment of brain development. To this purpose we first sought to establish whether Poly administered during the first two postnatal weeks improves neurogenesis in the hippocampal dentate gyrus (DG), a key developmental defect of DS, and, if so, to identify the optimum dose. To this purpose in a first group of mice we carried out pilot experiments. After having identified the optimum dose, we treated additional groups of mice with this dose to establish whether it was also able to improve dendritogenesis and spinogenesis and to clarify possible molecular mechanisms underlying the effects of Poly (Fig. 1A). Finally, in order to establish whether treatment translated into a behavioral benefit, we treated mice with the optimum dose of Poly up to adolescence (Fig 1B).

2.3. Experimental protocol

Mice used in this study derived from 39 litters. Treatment with either Polydatin (Poly) or vehicle (PBS) began on postnatal day 3 (P3). We treated all mice of each litter, with no specific selection criterion. The total number of mice treated with vehicle or Poly was 67 and 90, respectively. Mice are breastfed by their dams up to weaning (~P21). Since we were interested in evaluating the effect of different doses of Poly on brain development, Poly was not administered through breastfeeding but was injected directly into the pups. In a first group of mice we established the effects of different doses of Poly on the proliferation rate in the DG of Ts65Dn and control mice. Pups (euploid: n=15; Ts65Dn: n=19), received a daily subcutaneous injection (at 9-10 am) of different doses of Poly (Sigma15721, 0.625, 1.25, 2,5, 5.0, and 10.0 mg/kg in vehicle) from postnatal day 3 (P3) to P15. Age-matched euploid (n=5) and Ts65Dn (n=6) pups were injected with vehicle (Fig. 1A). On P15, mice received an intraperitoneal injection (150 μg/g body weight) of BrdU (5-bromo-2-deoxyuridine; Sigma), a marker of cells in the S-phase of the cell cycle (Nowakowski et al., 1989) in TrisHCl 50 mM 2h before being killed and the number of BrdU positive cells in the DG was evaluated in order to establish the optimum dose. The body weight of these mice was recorded every day. Brain weight was recorded after the sacrifice. In these pilot experiments we found that the dose that had the largest enhancing effects on hippocampal neural progenitor cells (NPCs) proliferation in

Ts65Dn mice was 2.5 mg/kg (see Fig. 2B,C). Therefore, further steps of our study were carried out using a 2.5 mg/kg dose. A second group of mice was treated with either vehicle or Poly 2.5 mg/kg from P3 to P15. Their right hemisphere was used for Golgi staining (vehicle-treated euploid mice: n=6, vehicle-treated Ts65Dn mice: n=5, Poly-treated euploid mice: n=5, Poly-treated Ts65Dn mice: n=4) and their left hemisphere was used for Ki-67 or cyclin D1 immunohistochemistry (IHC) (vehicle-treated euploid mice: n=4, vehicle-treated Ts65Dn mice: n=4, Poly-treated euploid mice: n=4, Poly-treated Ts65Dn mice: n=4). A third group of mice was treated with either vehicle or Poly 2.5 mg/kg from P3 to P15 and was used for western blotting (vehicle-treated euploid mice: n=11, vehicle-Ts65Dn mice: n=11, Poly-treated euploid mice: n=10, Poly-treated Ts65Dn mice: n=9). At P15, mice of all groups were killed, and their body and brain weight were recorded. The Ts65Dn strain is characterized by a high mortality rate during gestation (Roper et al., 2006). For this reason, the number of Ts65Dn pups in a litter result approximately 30% instead of the theoretical value of 50%. Moreover, Ts65Dn mice exhibit a high mortality rate before weaning (Roper et al., 2006). This means that numerous litters (26 litters) were needed in order to obtain a sufficiently large number of Ts65Dn mice. Due to this obstacle, we had a surplus of treated and untreated euploid mice. In order to numerically match euploid and Ts65Dn mice, we used only a part of the euploid mice. The latter were randomly chosen to avoid an experimental bias. The number and sex of mice used in the pilot experiments, for Golgi staining, Ki-67 and Cyclin D1 IHC and western blotting are detailed in Table 1, Table 2, and Table 3. A fourth group of mice derived from 7 litters (euploid: n=21, Ts65Dn: n=7), received a daily subcutaneous injection of 2.5 mg/kg Poly from P3 to P48-52 (Fig. 1B). Age-matched euploid (n=14) and Ts65Dn (n=9) mice derived from 6 litters were injected with vehicle. These mice were used to establish the effect of treatment on behavior at the end of treatment. The number and sex of these mice are detailed in Table 4. On P48-52, these mice were subjected to the Passive Avoidance (PA) test (see below). Treatment was continued during behavioral testing that lasted two days. These mice will be called hereafter P50 mice. At the end of the behavioral test, P50 mice were weighed and killed, their brains were removed and weighed. Mice that had received Poly will be called “treated mice”. Mice that had received the vehicle will be called “untreated mice”.

2.4. Histological procedures

2.4.1. BrdU immunohistochemistry and DAPI staining

The whole left hemisphere of P15 mice of the pilot experiments was cut coronally with a cryostat into 30-µm-

thick sections that were serially mounted (one out of six) on slides and used for BrdU IHC and DAPI staining, as described below. From each animal 4-5 series were obtained consisting each of six slides each of which contained 9-12 brain sections. To quantify the effect of Poly on the proliferation rate of NPCs, BrdU IHC was performed on sections covering the whole hippocampal region. Sections were incubated with rat anti-BrdU antibody (diluted 1:200; abcam ab6326). Detection of BrdU positive-cells was performed with a Cy3-conjugated anti-rat secondary antibody (diluted 1:200; Jackson Immunoresearch). For the study of the effect of treatment on the stereology of the DG, sections of P15 mice of the pilot experiments treated with 2.5 mg/kg Poly were stained with the fluorescent nuclear DNA stain DAPI (4′,6-diamidino-2-phenylindole; SouthernBiotech).

2.4.2. Immunohistochemistry for Ki-67 and Cyclin D1

The left hemisphere of P15 mice of group 2 was cut coronally with a freezing microtome into 30-μm-thick sections. To quantify the effect of Poly on the total number of proliferating cells in the DG, one out of six free-floating sections covering the whole hippocampal region were immunostained for Ki-67 (diluted 1:100; ThermoFisher Scientific). Detection was performed with Alexa Fluor 555 anti-rabbit secondary antibody (diluted 1:200; Invitrogen). Sections were counterstained with DAPI to label cell nuclei. To quantify the effect of Poly on the levels of Cyclin D1 in NPCs of the DG, one out of six free-floating sections from the rostral one third of the DG were subjected to immunohistochemistry for Cyclin D1 (diluted 1:100; Invitrogen). The endogenous peroxidase activity was inhibited using a methanol/H_2O_2 0.3% solution for 30 min in dark room. Antigens were retrieved with citrate buffer, pH 6.0 at 98°C for 15 min. After cooling at room temperature for 20min, sections were washed with distilled water. Detection was performed with an HRP-conjugated anti-rabbit secondary antibody (1:200; Jackson Immunoresearch) and DAB kit (Vector Laboratories). Negative controls for each tissue section were prepared without the primary antibody No immunoreactivity was evident in negative control sections.

2.4.3. Golgi staining

The right hemispheres of P15 mice of group 2 were immersed in the impregnation solution of the FD Rapid Golgi Stain ™ Kit (FD Neuro Technologies, Inc.) containing mercuric chloride, potassium dichromate and potassium chromate and were stored at room temperature in the dark for 2 weeks. Hemispheres were then transferred into Solution C of the same kit and stored at room temperature in the dark for at least 72 h. After these steps, hemispheres were cut with a microtome into 90-μm-thick coronal sections. Sections were mounted on gelatin-

coated slides and were air dried at room temperature in the dark for at least one day. After drying, sections were rinsed with distilled water and subsequently stained in the developing solution.

2.5. Measurements

2.5.1. Number of BrdU-positive cells

We evaluated the number of BrdU-positive cells in the DG of P15 mice treated with all tested doses of Poly (see above). In P15 mice treated with Poly 2.5 mg/kg, we additionally evaluated the number of BrdU-positive cells in the subventricular zone (SVZ) overlying the hippocampus (which corresponds to the caudal one half of the SVZ of the lateral ventricle), and in the retrosplenial cortex (RSC). Cells were counted using a fluorescence microscope (Nikon Eclipse; objective: x 20, 0.5 NA) in 1 out of 6 serial sections covering the whole rostral to caudal extent of the DG and caudal SVZ. Since in sections processed for BrdU immunohistochemistry it was not possible to delineate the RSC based on its cytoarchitectonic features, we used as reference the Allen's on-line mouse brain reference atlas (https://mouse.brain-map.org/experiment/thumbnails/100048576?image_type=atlas). The rostral and caudal borders of the RSC roughly correspond to the appearance of the DG (image 66 of the atlas) and disappearance of the presubiculum (image 98 of the atlas), respectively. The medial border of the RSC is at 1000-1200 μm from the brain midline (see Fig. 4A,B). In the RSC, we evaluated the number of BrdU-positive cells in seven serial (1 out of 6) sections taken starting from the appearance of the DG. With a section thickness of 30 μm and a sampling frequency of 1/6, the rostro-caudal length of the sampled RSC is of ~1260 μm, which roughly corresponds to the rostral one third of the RSC. In each sampled section, the perimeters of the regions of interest (ROI) were manually traced. In the case of the RSC, the traced area extended 1000 μm from the midline and covered the whole thickness of the RSC, white matter included (Fig. 4A,B). Within each ROI all labelled cells were counted using a modified unbiased stereology protocol that has previously been reported to successfully quantify BrdU labeling (Kempermann and Gage, 2002; Malberg et al., 2000; Tozuka et al., 2005). Cells were counted in the entire z axis (1 μm steps) in each section. The total number of BrdU-labeled cells counted in the series of sampled sections was multiplied by 6 (the inverse of the section sampling fraction: 1/6) to obtain the total estimated number of BrdU-positive cells in each ROI. In the DG and SVZ, the mean number of BrdU-positive

cells per section was additionally evaluated by averaging the number of cells counted in the series of sampled sections.

2.5.2. Number of Ki-67-positive cells

Ki-67-immunoreactive cells in the DG were counted using a fluorescence microscope (Nikon Eclipse; objective: x 20, 0.5 NA) in 1 out of 6 serial sections covering the whole rostral to caudal extent of the DG. Quantification of total cell number was carried out by using a modified unbiased stereology protocol (Kempermann and Gage, 2002; Malberg et al., 2000; Tozuka et al., 2005). The total number of Ki-67-labeled cells counted in the series of sampled sections was multiplied by 6 (the inverse of the section sampling fraction: 1/6) to obtain the total estimated number of Ki-67-positive cells.

2.5.3. Number of granule cells in the DG

Unbiased stereology of the DG was performed in DAPI-stained sections of P15 mice treated with 2.5 mg/kg Poly, starting from a random position of the first (rostral most) section plane. The optical disector method was used to obtain cell density, and the Cavalieri principle was used to estimate volume, as previously described (Stagni et al., 2019).

2.5.4. Cyclin D1 levels in NPCs of the DG

NPCs in the SGZ of the DG showed variable intensities of nuclear staining (see Fig. 8B). Intensity of Cyclin D1 immunoreactivity in individual NPCs was determined by optical densitometry. Bright field images were captured using a light microscope (final magnification 300 x). The contour of each cell was manually drawn and the optical density (OD) of each cell was evaluated using the Image Pro Plus (Media Cybernetics) tool “Histogram”. Since the granule neurons of the DG did not exhibit immunoreactivity for Cyclin D1 (see Fig. 8B), the OD in the granule cell layer was chosen as background and used to correct the OD of NPCs in individual section. In each mouse, 3-5 sections across the DG were analyzed and OD was evaluated in 70-140 NPCs per section. In each animal, the mean OD for Cyclin D1 was obtained by averaging the means of the sampled sections and expressed as multiple of the OD of untreated euploid mice.

2.5.5. Dendritic spine density

Spines of granule cells of the DG were counted live in Golgi-stained sections of P15 mice treated with 2.5 mg/kg Poly using a 100x oil immersion objective lens (Leitz microscope and objective with 1.4 NA). Spine density values

were evaluated in dendritic segments located in the inner (proximal dendrites) and outer (distal dendrites) half of the molecular layer. For each neuron, 3 proximal and 3 distal segments were analyzed. For each animal, spines were counted in at least 4/5 neurons. The length of each sampled dendritic segment was determined by tracing its profile and the number of spines was counted manually. The linear spine density was calculated by dividing the total number of spines by the length of the dendritic segment. Spine density was expressed as number of spines per 100 μm dendrite.

2.5.6. Measurement of the dendritic tree

The dendritic tree of granule cells of P15 mice was traced in the same Golgi-stained sections used for spine density evaluation (see preceding section). We used a dedicated software custom-designed for dendritic reconstruction (Immagini Computer di Maurizio Abbate & C. SNC, Bareggio, MI, Italy) interfaced with Image Pro Plus (Media Cybernetics). The dendritic tree was traced live, at a final magnification of 500x, by focusing into the depth of the section. The operator starts with branches emerging from the cell soma and after having drawn the first parent branch goes on with all daughter branches of the next order in a centrifugal direction. At the end of tracing, the program reconstructs the total dendritic length, the number of branches of each order, and the mean length of branches of each order. The dendritic tree was reconstructed in 7-10 neurons per animal. These data were averaged in order to obtain the mean value for each animal.

2.5.7. Western blotting

In homogenates of the hippocampal formation of P15 mice, total proteins were obtained as previously described (Trazzi et al., 2011). The following primary antibodies were used: anti-Cyclin D1 (1:1000, Invitrogen); anti-DSCAM (1:500, a gift from Dr Maria Luz Montesinos), and anti-α-Tubulin (1:1000, Sigma). Densitometric analysis of digitized images with ChemiDoc XRS+ was performed with Image Lab software (Bio-Rad Laboratories, Hercules, CA, USA) and intensity for each band was normalized to the intensity of the corresponding α-Tubulin band.

2.5.8. Passive Avoidance test

The passive avoidance test (PA) was used to examine learning and memory performance in P50 mice. For the PA we used a tilting-floor box (47x18x26 cm) divided into two compartments by a sliding door and a control unit

incorporating a shocker (Ugo Basile, Italy). This classic instrument for Pavlovian conditioning exploits the tendency in mice to escape from an illuminated area into a dark one (step-through method). On the first day mice were individually placed into the illuminated compartment. After 60 s of habituation period, the connecting door between the chambers opened. In general, mice step quickly through the gate and enter the dark compartment because mice prefer to be in the dark. Upon entering the dark compartment, mice received a brief foot shock (0.3 mA for 3 s) and were removed from the chamber after 15 s of latency. If the mouse remained in the light compartment for the duration of the trial (5 min), the door closed, and the mouse was removed from the light compartment. After a 24h retention period, the trial was repeated without a shock and the time it took them to re-enter the dark compartment (latency) was measured.

2.6. Statistical Analysis

Results are presented as mean ± standard error of the mean (SE). Data were analyzed with the IBM SPSS 22.0 software. Before running statistical analyses, we checked data distribution and homogeneity of variances for each variable using the Shapiro-Wilk test and Levene's test, respectively. If the data were normally distributed and variance was homogeneous, statistical analysis was carried out using either a one-way ANOVA or a two-way ANOVA with genotype (euploid, Ts65Dn) and treatment (Poly), as factors. *Post hoc* multiple comparisons were then carried out using Fisher's least significant difference (LSD) test. If the data were not normally distributed and variance was heterogeneous, transformations were made to achieve normality. If the transformed data did not achieve normality, statistical analysis was carried out using the Kruskal-Wallis test followed by the Mann–Whitney U test. Based on the "Box plot" tool available in SPSS Descriptive Statistics, in each analysis we excluded the extremes, i.e., values that were larger than 3 times the IQ range [$x \geq Q3 + 3 * (IQ)$; $x \leq Q1 - 3 * (IQ)$]. The number of mice included in (and excluded from, if any) individual analyses is reported in the legends of figures. A probability level of $p \leq 0.05$ was considered to be statistically significant.

3. RESULTS

3.1. Effect of treatment with Poly on neural precursor proliferation in the dentate gyrus of Ts65Dn and euploid mice

In order to establish whether Poly improves the typically reduced proliferation rate of NPCs in the DG of Ts65Dn mice and to find the optimum dose, we treated Ts65Dn and euploid pups with a series of doses of Poly. In view of the large bioavailability of Poly we thought that doses of Poly lower than the dose of resveratrol (20 mg/kg body weight) previously shown to increase neurogenesis (Kumar et al., 2016) should be sufficient to induce pro-proliferative effect. Thus, we first started at a dose of 10.0 mg/kg, and then progressively reduced the doses, each dose being one half of the preceding one (10.0, 5.0, 2.5, 1.25, and 0.625 mg/kg). At the end of a daily treatment from P3 to P15 with each dose, mice received one injection of BrdU and were killed after 2 h in order to examine the effect of treatment on the number of cells in the S phase of the cell cycle (proliferating NPCs) in the DG. We evaluated the effect of treatment both on total number of NPCs and mean number of NPCs per hippocampal section.

We first analyzed the effect of treatment separately in mice of each genotype treated with different doses of Poly, to reconstruct a dose-response curve. A one-way ANOVA on total number of BrdU-positive cells in the DG of Ts65Dn mice showed a significant effect of treatment [$F(5,24) = 15.037$, $p < 0.001$]. A *post hoc* Fisher's LSD test showed that all tested doses increased the total number of proliferating cells and that, in absolute terms, the 2.5 mg/kg dose had the highest pro-proliferative effect in comparison with the other doses (Fig. 2B). While in Ts65Dn mice that received 10.0 and 0.625 mg/kg Poly there was an increase in the number of proliferating NPCs of about +30% and +37%, respectively, in mice treated with 2.5 mg/kg Poly there was an increase of about +97%, i.e. there was nearly a doubling of NPC number. A one-way ANOVA on the mean number of BrdU-positive cells per section in the DG of Ts65Dn mice showed a significant effect of treatment [$F(5,24) = 5.873$, $p = 0.02$]. A *post hoc* Fisher's LSD test showed that the doses of 5.0, 2.5, and 1.25 mg/kg increased the mean number of proliferating cells per section, while the highest dose (10.0 mg/kg) and the lowest dose (0.625 mg/kg) had no effect (Fig. 2C). Again, in absolute terms, the 2.5 mg/kg dose had the largest effect (+74%) in comparison with the other doses (Fig. 2C).

A one-way ANOVA on the number of BrdU-positive cells in the DG of euploid mice showed a significant effect of treatment [$F(5,19) = 3.789$, $p = 0.022$]. A *post hoc* Fisher's LSD test showed that only the doses of 10.0, 5.0, and 2.5 mg/kg increased proliferation rate, whereas the doses of 1.25 and 0.625 mg/kg had no effect (Fig. 2D). A one-way ANOVA on the mean number of BrdU-positive cells per section in the DG of euploid mice showed no

significant effect of treatment. Therefore, data were not further analyzed (Fig. 2E).

Having found that Poly increased the proliferation potency of NPCs in the DG of Ts65Dn mice in comparison with their untreated counterparts, we were then interested in establishing whether this effect translated into restoration in the number of NPCs in comparison with untreated euploid mice. To this purpose, Ts65Dn mice that had received either vehicle or different doses of Poly were compared with euploid mice that had received vehicle only (Fig. 2F). A two-way ANOVA on the total number of BrdU-positive cells showed no genotype x treatment interaction, but a main effect of genotype [$F(1,29) = 12.022$, $p = 0.002$] and a main effect of treatment [$F(1,29) = 11.759$, $p < 0.001$]. A *post hoc* Fisher's LSD test showed that Ts65Dn mice had fewer BrdU-positive cells than euploid mice, as expected, and that in Ts65Dn mice treated with the doses of 10.0, 1.25, and 0.625 mg/kg Poly the total number of proliferating cells became similar to that of untreated euploid mice; interestingly in Ts65Dn mice treated with the doses of 5.0, and 2.5 mg/kg the number of proliferating cells became even larger in comparison with euploid mice (Fig. 2F). The Kruskal-Wallis test on the mean number of BrdU-positive cells per section revealed a difference between groups [$\chi2\ (6) = 15.039$, $p= 0.020$]. The Mann-Whitney tests, however, showed no differences between groups (Fig. 2G).

To establish the effect of Poly on the total number of NPCs in the DG we counted the number of cells positive for Ki-67, an endogenous marker expressed during the whole cell cycle, in mice treated with Poly 2.5 mg/kg and their untreated counterparts. A two-way ANOVA on the total number of Ki-67-positive cells showed no genotype x treatment interaction, but a main effect of genotype [$F(1,15) = 23.752$, $p < 0.001$] and a main effect of treatment [$F(1,15) = 19.885$, $p = 0.001$]. A *post hoc* Fisher's LSD test showed that treatment increased the number of Ki-67-positive cells both in euploid and Ts65Dn mice, indicating that treatment expands the size of the pool of NPCs in the DG (Fig. 2I).

Having found that in Ts65Dn mice 2.5 mg/kg Poly had the largest pro-neurogenic effect in the DG, we sought then to establish whether a similar effect took place in other neurogenic niches. To this purpose we counted the number of BrdU-positive cells in the SVZ and RSC.

3.2. Effect of treatment with Poly on neural precursor proliferation in the subventricular zone of Ts65Dn and euploid mice

A two-way ANOVA on the total number of BrdU-positive cells in the SVZ of P15 mice treated with 2.5 mg/kg Poly showed no genotype x treatment interaction, a main effect of genotype [$F(1,17) = 6.621$, $p = 0.022$], and a main effect of treatment [$F(1,17) = 17.340$, $p = 0.001$]. A *post hoc* Fisher's LSD test showed that Ts65Dn mice had fewer cells in comparison with untreated euploid mice (-30%). After treatment with Poly, Ts65Dn mice underwent an increase in the number of proliferating cells (+62%) that became similar to that of untreated euploid mice (Fig. 3B,C). In the SVZ of euploid mice, treatment caused an increase in the number of proliferating cells that became significantly larger (+27%) in comparison with that of their untreated counterparts (Fig. 3B,C).

A two-way ANOVA on the mean number of BrdU-positive cells per section showed no genotype x treatment interaction, no main effect of genotype but a main effect of treatment [$F(1,17) = 14.534$, $p = 0.002$]. A *post hoc* Fisher's LSD test showed that Ts65Dn mice had a reduced cell number per section in comparison with untreated euploid mice (-25%). After treatment with Poly, Ts65Dn mice underwent an increase in the total number of proliferating cells (+49%) that became similar to that of untreated euploid mice (Fig. 3B,D). In the SVZ of euploid mice, treatment caused an increase in the number of proliferating cells per section that became slightly larger (+14%) in comparison with that of their untreated counterparts although this effect was not statistically significant (Fig. 3B,D).

3.3. Effect of treatment with Poly on the proliferation rate in the retrosplenial cortex of Ts65Dn and euploid mice

Cells detached from the SVZ retain proliferative capacity during migration which allows one to follow their route (Brazel et al., 2003). In agreement with the radial migration of NPCs born in the SVZ, we found BrdU-positive cells in the white matter and cortex overlying the SVZ of P15 mice. BrdU-positive cells appeared more numerous in the RSC, which is in agreement with the later development of this cortical region (Zgraggen et al., 2012). Considering the relevance of the RSC in some types of memories that are compromised in DS (Vann and Aggleton, 2002), we deemed it of interest to evaluate the proliferation potency also in this region. A two-way ANOVA on the total number of BrdU-positive cells in the RSC of P15 mice treated with 2.5 mg/kg Poly showed no genotype x treatment interaction, no main effect of genotype but a main effect of treatment [$F(1,17) = 11.307$, $p = 0.005$]. A *post hoc* Fisher's LSD test showed that Ts65Dn mice had a reduced number of proliferating cells in

comparison with untreated euploid mice (-38%). After treatment with Poly, Ts65Dn mice underwent an increase in the number of proliferating cells (+102%) that became similar to that of untreated euploid mice (Fig. 4C,D). In the RSC of euploid mice, treatment caused an increase in the number of proliferating cells that became larger (+23%) in comparison with that of their untreated counterparts, although this difference was not statistically significant (Fig. 4C,D).

3.4. Effect of Poly on the number of granule neurons in the dentate gyrus of Ts65Dn and euploid mice

Since neonatal treatment with the dose of 2.5 mg/kg of Poly induced a large increase in the proliferation potency of NPCs in the DG, we sought to establish whether this effect translated into an improvement or even restoration of the defective cellularity that characterizes the granule cell layer of the DG in trisomic pups (Bianchi et al., 2010; Giacomini et al., 2015; Stagni et al., 2016; Stagni et al., 2017; Stagni et al., 2019). To this purpose, the DG of vehicle treated euploid and Ts65Dn mice and euploid and Ts65Dn mice treated with 2.5 mg/kg Poly in the period P3-P15 was subjected to stereological analysis.

A two-way ANOVA on the volume of the granule cell layer showed no genotype x treatment interaction but revealed a main effect of genotype [$F(1,17) = 9.525$, $p \leq 0.008$] and a main effect of treatment [$F(1,17) = 6.552$, $p = 0.023$]. A *post hoc* Fisher's LSD test showed that the granule cell layer of untreated Ts65Dn mice had a reduced volume in comparison with euploid mice and that treatment restored its value to the euploid level (Fig. 5B). Unlike in Ts65Dn mice, in euploid mice treatment had no effect on the volume of granule cell layer (Fig. 5B). A two-way ANOVA on granule cell density showed no genotype x treatment interaction, no main effect of genotype and no main effect of treatment. Therefore, data were not further analyzed. A two-way ANOVA on the total number of granule cells showed no genotype x treatment interaction but showed a main effect of genotype [$F(1,17) = 4.767$, $p \leq 0.047$] and a main effect of treatment [$F(1,17) = 4.826$, $p = 0.045$]. A *post hoc* Fisher's LSD test showed that untreated Ts65Dn mice had a reduced number of granule cells in comparison with untreated euploid mice and that treatment increased its value that became similar to that of untreated euploid mice (Fig. 5D).

These results indicate that the increase in the proliferation potency of granule cell precursors induced by neonatal treatment with 2.5 mg/kg Poly in Ts65Dn mice reinstates the development of the granule cell layer in terms of volume and total granule cell number.

3.5. Effect of Poly on dendritic spine density in the dentate gyrus of Ts65Dn and euploid mice

In order to establish whether Poly improves the typical spine density reduction that characterizes trisomic pups (Giacomini et al., 2015; Stagni et al., 2016; Stagni et al., 2017; Stagni et al., 2019), in Golgi-stained brains we evaluated spine density on the dendritic arbor of the granule neurons. Spine density was evaluated separately in dendritic branches harbored in the inner and outer half of the molecular layer, which are receptive fields of different inputs to the granule neurons (Amaral and Witter, 1995). The representative images of proximal dendritic branches reported in Fig. 6A show that the typical spine paucity in Ts65Dn mice was largely improved following treatment with Poly. The Kruskal-Wallis test on proximal spine density revealed a difference between groups [$\chi 2$ (3) = 9.629, p= 0.022]. The Mann-Whitney tests showed a significantly reduced spine density in untreated Ts65Dn mice in comparison with untreated euploid mice and that in treated Ts65Dn mice there was a spine density increase so that their number became similar to that of untreated euploid mice (Fig. 6B). The Kruskal-Wallis test on spine density on distal dendritic segments revealed a difference between groups [$\chi 2$ (3) = 12.071, p= 0.007]. The Mann-Whitney tests showed a reduced spine density in untreated Ts65Dn mice in comparison with untreated euploid mice and that in Ts65Dn mice treated with Poly there was a spine density increase so that their number became similar to those of untreated euploid mice (Fig. 6C). In euploid mice, unlike in Ts65Dn mice, treatment with Poly had no effect on spine density on neither proximal nor distal dendritic branches (Fig, 6A-C).

These results show that Poly fully restores dendritic spine density along the whole dendritic tree of the granule neurons of Ts65Dn mice but does not increase spine density in euploid mice.

3.6. Effect of Poly on the dendritic architecture of the granule neurons of Ts65Dn and euploid mice

In order to establish whether Poly is able to foster dendritic development, we quantified the dendritic arbor of granule neurons in terms of total number of branches and total length as well as in terms of number and length of branches of the different orders.

A two-way ANOVA on total dendritic length showed a genotype x treatment interaction [$F(1,19) = 20.115$, $p < 0.001$], a main effect of genotype [$F(1,19) = 5.502$, $p = 0.032$], and a main effect of treatment [$F(1,19) = 12.256$, $p = 0.003$]. A *post hoc* Fisher's LSD test showed that the total dendritic length of untreated Ts65Dn mice

was significantly reduced (-27%) in comparison with that of untreated euploid mice (Fig. 7A). Treatment with Poly caused an increment in total dendritic length of Ts65Dn mice (+43% vs. untreated Ts65Dn mice) that became similar to that of untreated euploid mice (Fig. 7A). In euploid mice treatment with Poly had no effect on total dendritic length (Fig. 7A).

A two-way ANOVA on total number of dendritic branches showed a genotype x treatment interaction [$F(1,19) = 10.934$, $p = 0.004$], no main effect of genotype, but a main effect of treatment [$F(1,19) = 24.736$, $p < 0.001$]. A *post hoc* Fisher's LSD test showed that total number of dendritic branches of untreated Ts65Dn mice was significantly reduced (-40%) in comparison with that of untreated euploid mice (Fig. 7B). Treatment with Poly caused an increment in total number of branches of Ts65Dn mice (+82% vs. untreated Ts65Dn mice) that became even larger (+20%) than that of untreated euploid mice (Fig. 7B). In euploid mice treatment with Poly had no effect on total number of dendritic branches (Fig. 7B).

In order to dissect the effect of treatment on details of the dendritic architecture, we examined each dendritic order separately. Regarding the number of dendritic branches of individual orders, a *post hoc* Fisher's LSD test (after two-way ANOVA) showed that untreated Ts65Dn mice had a similar number of branches of orders 1 and 2 as untreated euploid mice but fewer branches of orders 3–5 (Fig. 7C). Moreover, unlike euploid mice, they lacked branches of order 6 (Fig. 7C, black arrow). In Ts65Dn mice treated with Poly the number of branches of orders 3-5 increased and became similar to that of untreated euploid mice. In addition, there was a *de novo* appearance of branches of order 6. In euploid mice, treatment with Poly had no effect on the number of branches of any order (Fig. 7C). Regarding the mean length of dendritic branches of individual orders, a *post hoc* Fisher's LSD test (after two-way ANOVA) showed that in untreated Ts65Dn mice the branches of order 1 and 2 were notably longer in comparison with untreated euploid mice (Fig. 7D). This is consistent with previous evidence in P15 (Stagni et al., 2019) and adult (Guidi et al., 2013; Stagni et al., 2015b) Ts65Dn mice. Ts65Dn mice treated with Poly underwent a reduction in the excessive length of branches of order 1 and 2 that became similar to that of untreated euploid mice (Fig. 7D). No difference was found in the mean length of branches of orders 3-5 in untreated Ts65Dn mice as compared with untreated euploid mice (Fig. 7D). Treatment had no effect on the length of branches of orders 4-6 of Ts65Dn mice in comparison with untreated euploid mice but caused a reduction in the length of branches of orders 3 (Fig. 7D). In euploid mice treatment had no effect on the mean length of branches

of any order except for branches of order 2 and 3, that underwent a length reduction in comparison with those of untreated euploid mice (Fig. 7D). The overall effect of genotype and treatment on the dendritic architecture of the granule cells can be appreciated at a glance looking at the dendrograms reported in Fig. 7E.

These results indicate that the dendritic arbor of the granule neurons of Ts65Dn mice had a reduced total length due to a reduction in the number, but not length, of individual dendritic branches. Indeed, branches of orders 1 and 2 had a greater length in comparison with those of euploid mice but this increase was largely offset by a notable reduction in the number of branches of order > 2. Treatment with Poly was able to fully restore total dendritic length in Ts65Dn mice. This effect was not due to an increase in the length of individual branches but to an increase in the abundance of branches of orders 3-5 and the appearance of branches of order 6. Thus, although treatment reduced the lengths of branches of orders 1-3 this effect was counterbalanced by the increase in the number of branches of higher orders. In euploid mice the dendritic architecture was almost unchanged by treatment with Poly. This finding in conjunction with the absence of any effect on spine density indicates that Poly exerts no beneficial effects on dendritic development in the normal brain, at least at the tested dose.

3.7. Effect of Poly on Cyclin D1 expression in Ts65Dn and euploid pups

Cell cycle alterations are key determinants of the reduced proliferation potency that characterizes DS and reduced levels of Cyclin D1, a key cell cycle regulator, appear to be a common denominator whereby various triplicated genes may impair proliferation of trisomic NPCs (see (Stagni and Bartesaghi, 2022; Stagni et al., 2018)). Thus, we carried out western blotting experiments on hippocampal extracts from P15 mice to establish whether the proliferation enhancement induced by treatment with Poly was associated with changes in Cyclin D1 protein levels. The Kruskal-Wallis test on Cyclin D1 expression revealed a marginally significant difference between groups [$\chi 2$ (3) = 7.594, p= 0.055]. The Mann-Whitney tests showed a significantly reduced Cyclin D1 expression in untreated Ts65Dn mice in comparison with untreated euploid mice (Fig. 8A). In Ts65Dn mice treated with Poly there was an increase in Cyclin D1 levels in comparison with their untreated counterparts, although this difference was not statistically significant. After treatment with Poly, however, Ts65Dn mice showed no longer a difference in Cyclin D1 levels in comparison with untreated euploid mice (Fig. 8A), suggesting that treatment had normalized its expression. No effect of treatment with Poly were found in euploid mice (Fig. 8A).

The genotype and treatment related changes in Cyclin D1 levels found in western blotting might be due to either differences in the number of NPCs or to changes in Cyclin D1 levels in individual NPCs. To clarify this issue, we evaluated the levels of Cyclin D1 in individual NPCs of the SGZ through OD analysis. A two-way ANOVA on Cyclin D1 levels showed a genotype x treatment interaction [$F(1,15) = 7.023$, $p = 0.021$], a main effect of genotype [$F(1,15) = 4.568$, $p = 0.05$] and a main effect of treatment [$F(1,15) = 11.693$, $p = 0.005$]. A *post hoc* Fisher's LSD test showed significantly reduced Cyclin D1 levels in NPCs of untreated Ts65Dn mice in comparison with untreated euploid mice (Fig. 8B). In Ts65Dn mice treated with Poly, Cyclin D1 levels underwent an increase and became similar to those of untreated euploid mice (Fig. 8B). These findings indicate that the reduced levels of Cyclin D1 in NPCs of Ts65Dn mice are restored by treatment with Poly.

3.8. Effect of Poly on DSCAM expression in Ts65Dn and euploid mice

Down syndrome cell adhesion molecule (*DSCAM*) is a gene located on the so-called critical region of Chr21, a region that was previously thought to be particularly relevant for the DS-linked phenotypes. *DSCAM* expression is increased in neurospheres from fetuses with DS (Bahn et al., 2002), and children and adults with DS exhibit higher brain DSCAM levels (Saito et al., 2000) compared to controls. DSCAM is critically involved in dendrite morphology and connectivity (Fuerst et al., 2008) because it appears to suppress dendritic branching and spine formation (see Discussion for further details). Thus, overexpression of DSCAM may be a determinant of the impairment of dendritic maturation that characterizes DS. Confirming this idea, we previously found that DSCAM is overexpressed in the hippocampus of Ts65Dn mice and that treatment with fluoxetine normalized its levels, in conjunction with restoration of dendritic development (Guidi et al., 2013). Therefore, we carried out here western blot analysis on hippocampal extracts from P15 mice in order to confirm previous findings and to establish, additionally, whether the positive effects of Poly on the dendritic growth were associated with changes in DSCAM expression. A two-way ANOVA on DSCAM expression showed a marginally significant genotype x treatment interaction [$F(1,36) = 3.535$, $p = 0.069$], no main effect of genotype, but showed a main effect of treatment [$F(1,36) = 4.360$, $p < 0.045$]. A *post hoc* Fisher's LSD tests showed that untreated Ts65Dn mice had significantly higher levels of DSCAM in comparison with euploid mice (> 1.6 x) and that treatment with Poly normalized DSCAM

expression to euploid levels (Fig. 8B). No effect of treatment with Poly was found in euploid mice (Fig. 8B).

3.9. Effect of Poly on hippocampus-dependent memory in Ts65Dn and euploid mice

To establish whether the positive effects induced by Poly on the hippocampus translate into an improvement in hippocampus-dependent memory, mice were treated with Poly 2.5 mg/kg from P3 to ~P50 and subjected to the passive avoidance (PA) test during the last two days of treatment. In this test an animal is conditioned with a single aversive event and is later tested for recollection of that experience. Fig. 9 reports the latency time to enter the dark compartment on the first day (training) and on the second day (test) of the behavioral procedure for treated and untreated Ts65Dn and treated and untreated euploid mice. On the first day, all groups showed similar step-through latencies (Fig. 9A). After 24h (second day), animals were re-placed in the test apparatus to test their memory. The Kruskal-Wallis test on the second day latency revealed a significant difference between groups [$\chi 2$ (3) = 11.151, p= 0.011]. The Mann-Whitney tests showed that untreated Ts65Dn mice were severely impaired in this task as shown by a reduced latency to enter the dark compartment in comparison with euploid mice (Fig. 9B). In treated Ts65Dn mice the latency underwent an increase and was no longer different in comparison with that of euploid mice (Fig. 9B) indicating that treatment had restored hippocampus-dependent memory. No effect of treatment was found in euploid mice (Fig. 9B).

3.10. General effects of treatment with Poly in Ts65Dn and euploid mice

Although an acute toxicology test in mice by oral administration of Poly 5000 mg/kg showed no behavioral changes or deaths (Ni et al., 2017) we deemed it of relevance to evaluate the body and brain weight of P15 (Fig 10A-F) and P50 (Fig. 10G,H) mice to establish whether a continuous treatment even at lower dose may adversely affect the body and brain growth.

A one-way ANOVA on the body weight of P15 Ts65Dn mice treated with either vehicle or different doses of Poly showed a significant effect of treatment [$F(5,53) = 3.030$, $p < 0.019$]. *Post hoc* LSD test showed no differences between treated and untreated Ts65Dn save for mice treated with Poly 5.0 mg/kg that had a body weight larger than untreated Ts65Dn mice (Fig, 10A). A one-way ANOVA on the brain weight of P15 Ts65Dn

mice showed no significant effect of treatment. Therefore, we did not further analyze these data (Fig. 10B).

A one-way ANOVA on the body weight of P15 euploid mice treated with either vehicle or different doses of Poly showed a significant effect of treatment [$F(5,51) = 3.252$, $p < 0.013$]. *Post hoc* LSD test showed that mice treated with Poly 2.5 mg/kg but not mice treated with the other doses had a body weight lower than untreated euploid mice (Fig. 10C). The Kruskal-Wallis test on the brain weight of euploid mice revealed a significant difference between groups [$\chi2$ (5) = 11.767, p= 0.038]. The Mann-Whitney tests showed a significantly reduced brain weight in euploid mice treated with the doses of 10.0 mg/kg and 2.5 mg/kg Poly in comparison with untreated euploid mice (Fig. 10D).

A two-way ANOVA on the body weight of P15 euploid and Ts65Dn mice treated with either vehicle or Poly 2.5 mg/kg showed no genotype x treatment interaction, but showed a significant effect of genotype [$F(1,78) = 14.914$, $p < 0.000$], and treatment [$F(1,78) = 6.043$, $p < 0.016$]. A *post hoc* Fisher's LSD test showed that untreated and treated Ts65Dn mice had a reduced body weight in comparison with untreated euploid mice and that a body weight reduction was present in treated vs. untreated euploid mice (Fig. 10E). The Kruskal-Wallis test on the brain weight of P15 mice treated with either vehicle or Poly 2.5 mg/kg revealed a significant difference between groups [$\chi2$ (2) = 9.456, p= 0.009]. The Mann-Whitney tests showed that untreated but not treated Ts65Dn mice had a reduced brain weight in comparison with untreated euploid mice and that a brain weight reduction was present in treated vs. untreated euploid mice (Fig. 10F).

The Kruskal-Wallis test on the body weight of P50 mice treated with either vehicle or Poly 2.5 mg/kg revealed a marginally significant difference between groups [$\chi2$ (3) = 7.076, p= 0.070]. The Mann-Whitney test showed that untreated Ts65Dn mice had a reduced body weight in comparison with euploid mic but that this difference was no longer present in treated Ts65Dn mice (Fig. 10G). A two-way ANOVA on the brain weight of P50 mice showed no genotype x treatment interaction, no main effect of genotype and no main effect of treatment (Fig. 10H).

These data, in accord with a large body of evidence, show that untreated Ts65Dn mice have a reduced body and brain weight in comparison with euploid mice in infancy (P15) and a reduced body weight in adolescence (P50) (Fig. 10E-G). The finding that in P15 Ts65Dn mice none of the tested doses of Poly further reduced their body and brain weight (Fig. 10A,B) indicates that treatment does not impair general health. This seems of

relevance because Ts65Dn mice are more fragile in comparison with euploid mice (Roper et al., 2006). Results additionally show that a prolonged treatment with Poly (from P3 to ~P50) was even followed by restoration of the body and brain weight of Ts65Dn mice (Fig. 10G,H), emphasizing the safety of a treatment with Poly. It must be noted that in P15 euploid mice Poly could negatively affect the body and brain weight (Fig. 10C,D), although this did not happen in P50 euploid mice (Fig. 10G,H). This suggests that, contrary to what might be expected, Poly may not be totally safe in euploid mice, at least in infancy.

4. DISCUSSION

4.1. Polydatin is a powerful neurogenesis enhancer in Ts65Dn mice

In NPC cultures, resveratrol appears to enhance proliferation at low concentrations but has inhibitory effects at high concentrations (Kumar et al., 2016). To establish potentially adverse effects of Poly, we tested here a wide range of doses (1:16). None of the tested doses had inhibitory effects on the proliferation potency of hippocampal NPCs both in euploid and Ts65Dn mice and in Ts65Dn mice all tested doses enhanced proliferation. It seems of relevance to note that the lowest dose tested here (0.625 mg/kg) is 32 times smaller than the dose of resveratrol (20 mg/kg) proven to be effective in vivo (Kumar et al., 2016), highlighting the advantage of Poly as a neurogenesis enhancer. The magnitude of the effect of Poly was dose-dependent and had maximum efficacy at a dose of 2.5 mg/kg body weight (Fig. 2B,C). While the doses of 0.625, 1.25, and 10.0 mg/kg were sufficient to restore NPC proliferation in the DG of Ts65Dn mice to the levels of euploid mice, the doses of 2.5 and 5.0 mg/kg increased the number of proliferating cells to levels even larger than those of untreated euploid mice (Fig. 2F). Importantly, in Ts65Dn mice the dose of 2.5 mg/kg was also able to enhance the proliferation rate in the SVZ (Fig. 3C,D), indicating that Poly fosters the proliferation of two different populations of NPCs, those in the DG and those in the SVZ. Poly was also able to increase the number of proliferating cells in the RSC (Fig. 4D). This effect may be attributable to an increase in the number of cells migrating from the SVZ to the RSC and/or to a direct pro-neurogenic effect of Poly on migrating cells.

The wide scope of action of Poly on different populations of proliferating cells found here in Ts65Dn mice suggests that Poly may represent an excellent treatment to counteract the widespread effects of DS on neurogenesis

and, thus, positively impact on different brain functions. Accordingly, we found that in Ts65Dn treated with Poly the reinstatement of hippocampal neurogenesis was accompanied by restoration of hippocampus-dependent memory (further discussed below). NPCs in the postnatal SVZ give origin to granule neurons destined to the olfactory bulb and glial cells (astrocytes and oligodendrocytes) destined to the cortical white and grey matter (Brazel et al., 2003). It would be of interest to establish whether the increase in the proliferation potency of NPCs in the SVZ of treated Ts65Dn mice leads to an increase in the number of granule neurons directed to the olfactory bulb and of oligodendrocytes migrating to the cortex. If so, the outcome might be an improvement in smell and myelination, two functions that are compromised in DS (Nijjar and Murphy, 2002; Olmos-Serrano et al., 2016).

Unlike in Ts65Dn mice, in euploid mice, the lower tested doses of Poly (0.625 and 1.5 mg/kg) were unable to increase hippocampal NPC proliferation, but the dose of 2.5 mg/kg and higher doses were able to enhance cell proliferation in the DG (Fig. 2D). The dose of 2.5 mg/kg was additionally able to enhance NPC proliferation in the SVZ (Fig. 3C). These findings indicate that Poly also fosters proliferation in the normal brain and suggest that treatment with Poly may be exploited to counteract the proliferation decline due to age or other adverse conditions in the general population.

4.2. Polydatin restores cellularity in the dentate gyrus of Ts65Dn mice

We found that in Ts65Dn mice treated with Poly from P3 to P15 the total number of granule neurons of the DG became similar to that of untreated euploid mice (Fig 5D), indicating that the increased proliferation rate of NPCs induced by Poly translates into an increase in neurogenesis. The increase in total number of granule cells was accompanied by an increase in the volume of the granule cell layer, but not by an increase in the density of granule cells. Although treatment with a dose of 2.5 mg/kg Poly enhanced NPC proliferation in the DG of euploid mice**,** a very moderate and not statistically significant increase in total granule cell number was detectable (Fig. 5D). This indicates that despite the pro-neurogenic effect of this dose of Poly in euploid mice, the outcome on cellularity was marginal or even absent. It seems likely that in the normal brain a ceiling effect prevents an increase in granule cell number above a preset level.

4.3. Cyclin D1 expression normalization may underlie restoration of neurogenesis in Ts65Dn mice

The genetic causes of reduced neurogenesis in DS are elusive and most likely multifaceted. Yet, accumulating evidence suggests that a reduction in Cyclin D1 levels and/or expression may be a key determinant of neurogenesis impairment and that various triplicated genes, including *DYRK1A*, *APP*, *RCAN1,* concur to this effect (see (Stagni and Bartesaghi, 2022; Stagni et al., 2018)). We found here that Ts65Dn mice had reduced hippocampal levels of Cyclin D1 in comparison with euploid mice, which fits with studies from various laboratories (see (Stagni and Bartesaghi, 2022; Stagni et al., 2018)) and that these differences were attributable to reduced levels of Cyclin D1 in individual NPCs. Importantly, after treatment with Poly, Cyclin D1 levels became similar to those of euploid mice, strongly suggesting that the neurogenesis increase induced by Poly in Ts65Dn mice may be mediated by Cyclin D1 (Fig. 8A). The mechanism whereby Poly modulates Cyclin D1 expression in DS needs specific investigations. Yet, some speculations can be attempted based on the literature. The effects of flavonoids on neurogenesis have been connected with modifications of CREB (see (Heberden, 2016)) and it is known that resveratrol, the cognate compound of Poly, activates the MAPK signaling pathway ending up with a subsequent increase in p-CREB expression (Kumar et al., 2016). CREB is a ubiquitous transcription factor, highly expressed in the brain in which it is involved in many signaling pathways. Once phosphorylated, CREB enters the nucleus where it binds to the CREB response element. Considering that CREB increases the expression of proliferation-related genes, including Cyclin D1 (Chen et al., 2019; Pawlonka et al., 2021; Yan et al., 2013), it seems likely that the increase in Cyclin D1 levels following Poly treatment may be mediated CREB phosphorylation. Although Cyclin D1 is a good candidate, it cannot be ruled out that mechanisms beyond Cyclin D1 are engaged by treatment with Poly. Indeed, in treated euploid mice there was no increase in Cyclin D1 levels although treatment increased the proliferation rate of NPCs in the DG and SVZ. This suggests that Poly may act on other pathways involved in the regulation of neurogenesis.

4.4. Restoration of DSCAM levels following treatment with Poly may underlie restoration of dendritic development in Ts65Dn mice

Confirming a previous study (Guidi et al., 2013), we found here that Ts65Dn mice exhibit a higher hippocampal expression of DSCAM (Fig. 8B). Research shows that in DSCAM mutant mice there is an increase

in the number of dendritic branches and spine density (Maynard and Stein, 2012). DSCAM deletion promotes dendritic outgrowth in the retina (Simmons et al., 2017), DSCAM down regulation increases the dendritic complexity of cortical neurons (Zhang et al., 2015), and DSCAM knockout or knockdown in pyramidal neurons leads to increased dendritic spine maturation (Chen et al., 2022). This evidence clearly indicates that DSCAM represses two key processes of dendritic maturation, i.e. dendritic arborization and spine formation. Therefore, its over expression in Ts65Dn mice can explain the abnormally long low-order dendritic branches and the paucity of higher order branches as well as the reduction in spine density of granule neurons. The finding that restoration of dendritic arborization and spine density following treatment with Poly went in tandem with a reduction of DSCAM expression (Fig. 8B) confirms the hypothesis that overexpression of DSCAM is a key determinant of dendritic abnormalities in DS. Interestingly, suppression of DSCAM signaling also reverses neurogenesis deficits in iPSC-derived cerebral organoids from patients with Down syndrome (Tang et al., 2021), suggesting that the reduction of DSCAM levels in Ts65Dn mice treated with Poly may contribute to increase neurogenesis. In addition, since DSCAM overexpression also impairs neuron migration (Mitsogiannis et al., 2020), down regulation of its expression may contribute to the increase in the number of migrating cells found here in the RSC of treated Ts65Dn mice.

Some investigations have shed light on mechanisms regulating DSCAM expression in DS. It has been shown that in the Ts1Cje DS model DSCAM mRNA is translated at dendritic level through an NMDA-dependent mechanism. NMDA receptor activation increases dendritic levels of DSCAM protein, while NMDA receptor inhibition has an opposite effect (Alves-Sampaio et al., 2010). There is evidence that Poly decreases the expression of subunit NR2B of the NMDA receptor in a model of alcohol-related dementia (Xu et al., 2011). Its cognate compound, resveratrol, down-regulates subunits NR1 and NR2B (Tsai et al., 2012), exerts inhibitory effects on NR1/NR2B receptor subunits (Hsieh et al., 2021) and its intravenous administration (2 mg/kg) inhibits NMDA

receptors function (Takehana et al., 2017). Based on these data, it is possible that Poly down-regulates DSCAM expression in Ts65Dn mice by modulating the activity of the NMDA receptors.

4.5. Treatment with Poly restores hippocampus-dependent memory in Ts65Dn mice

The hippocampal formation (DG plus fields CA3 and CA1) is fundamental for long-term declarative memory functions. Neocortical signals converging into the entorhinal cortex are relayed by the latter to the DG. Signals from the DG are then sequentially processed by field CA3, field CA1 (the so called "lamellar circuit") and finally fed back to the entorhinal cortex itself (Amaral and Witter, 1989; Sloviter and Lømo, 2012). Processing of signals along this reverberating circuit underlies long-term declarative memory functions. The paucity of granule neurons that characterizes DS is likely to be a key determinant of the impairment of long-term memory that characterizes DS. Moreover, the severe dendritic hypotrophy and spine density reduction seen in the Ts65Dn DS model suggests that these defects also play a key role in memory impairment.

The current study showed that treatment with Poly restored the total number of granule cells as well as total number and length of their dendritic branches, and dendritic spine density. The effects on spine density involved proximal and distal dendritic branches, suggesting restoration of overall connectivity. The middle and outer thirds of the dendritic tree of the granule cells receive signals from the entorhinal cortex and the inner third is host to inputs from the mossy cells that provide longitudinal "translamellar" connections (Amaral et al., 2007) which are thought to coordinate the activity of different "lamellae". In the light of the restorative effects of Poly on both granule cell number and overall dendritic development, an improvement in hippocampus-dependent memory is expected. Indeed, we found that Ts65Dn mice that had been treated with Poly from P3 to ~P50 (an age corresponding to late adolescence) (Laviola et al., 2003) exhibited restoration of hippocampus-dependent memory as assessed with the PA test (Fig. 9B).

5. CONCLUSIONS AND PERSPECTIVES

Our study shows that early postnatal treatment with Poly restores both neurogenesis and dendritogenesis impairments, the two major neurodevelopmental defects of DS. Importantly, the outcome was restoration of

hippocampus-dependent memory, indicating that these neuroanatomical effects were functionally effective. We tested here the effect of Poly in the early postnatal period because we wanted to establish whether both major neurodevelopmental defects of DS can be rescued. Considering the time course of neurogenesis and dendritogenesis in humans, the optimum time windows for treatment would be the prenatal period, for the improvement of neurogenesis, and the neonatal period, for the improvement of dendritogenesis. It must be noted, however, that the human use even of natural substances, such as Poly, during the delicate perinatal period may raise ethical issues due to possible side effects. In this connection, it seems of relevance to stress that Poly elicited positive effects on neurogenesis and dendritogenesis at very low doses. It can be estimated that the equivalent dose of 2.5 mg/kg/die in mice would be of 0.3 mg/kg/die for children and 0.2 mg/kg/die for adults, respectively (Reagan-Shaw et al., 2008). This means a total daily intake of 3 mg for a child weighing 10 kg and of ~14 mg for an adult weighing 70 kg. An intake of 14 mg/die is 6 times lower than the dose of 40 mg twice daily (i.e. 80 mg/die) that was shown to ameliorate liver injury and cognition in alcoholic patients (Pace et al., 2015).

There is scarce information in the literature regarding the toxicity and safety of Poly. We found here that neither a short (from P3 to P15) nor a prolonged (from P3 to ~ P50) treatment with Poly had adverse effects on body and brain weight of Ts65Dn mice (Fig. 10), although we cannot rule out that treatment might cause more subtle side effects on specific organs and functions. A recent preclinical study has examined the toxicology of Poly in a zebrafish model showing no toxicity of Poly up to 435 μM and that in zebrafish embryos exposed to Poly i) there were no developmental alterations; ii) there was no significant mortality, iii) there were no teratogenic effects, neurotoxicity, and cardiotoxicity (Schimith et al., 2024). In adolescent mice, after two weeks of Poly treatment (50/mg/kg/day) there are no detectable lesions in major thoracic organs (heart and lung) or abdominal organs (liver, kidney and spleen), suggesting a low cytotoxicity and favorable biosafety to tissues (Chen et al., 2020). Regarding safety in humans, Poly has been approved by the Sino Food and Drug Administration for clinical trials that entered stage II (see (Zeng et al., 2015)). A handful of clinical studies have examined the effects of Poly in a variety of disorders (see (Cherian et al., 2023; Şöhretoğlu et al., 2018)). Although most of these studies do not provide explicit information on the safety of treatment, two studies specify that treatment with Poly for a three-weeks period was safe both in pediatric and adult patients (Cremon et al., 2017; Di Nardo et al., 2024) and one

study reports no adverse events attributable to treatment with Poly for six months (Cervigni et al., 2019). In view of the paucity of clinical studies, the potential safety hazard of Poly remains to be better characterized for further clinical practices.

The efficacy of Poly in a DS model prospect the possibility of its use during early life stages for amelioration of DS-linked neurodevelopmental alterations. Additional research in DS models is needed to establish whether Poly is also effective during pregnancy, to clarify the duration of its effects on brain anatomy and behavior and to validate its safety. We hope that our findings will prompt additional research whose results may provide a solid basis for the design of clinical trials in infancy and, possibly, during pregnancy.

Conflict of interest

The authors declare that they have no conflict of interest.

Acknowledgments. This work was supported by a grant to R. B. from "Fondazione Generali" e "Assicurazione Generali", Italy. We thank Dr. Anna Rosa Vacca and Dr. Daniela Valenti for having prompted us to test the effects of polydatin in the Ts65Dn model. We express our gratitude to Prof. Roberto Rimondini for the use of his Passive Avoidance apparatus.

Author contribution.

M. E. Investigation, Formal analysis, Writing - review & editing. **F. S**. Data curation, Investigation, Writing - review & editing. **C. R.** Contributed to Investigation and Formal analysis. **L. A.** Contributed to Investigation and Formal analysis. **S. G**. Data curation, Investigation, Writing - review & editing. **R. B.** Conceptualization and study design, Funding acquisition, Investigation, Methodology, Supervision, Writing - review & editing.

Data Availability

The data that support the findings of this study are available from the corresponding author upon reasonable request.

REFERENCES

Altman, J. and Bayer, S., 1975. Postnatal development of the hippocampal dentate gyrus under normal and experimental conditions. In: Isaacson RL and Pribram KH, editors. The hippocampus, Vol 1. Plenum Press, New York and London. p 95-122.**,** 95-122.

Altman, J. and Bayer, S. A., 1990a. Migration and distribution of two populations of hippocampal granule cell precursors during the perinatal and postnatal periods. J Comp Neurol 301**,** 365-381.

Altman, J. and Bayer, S. A., 1990b. Mosaic organization of the hippocampal neuroepithelium and the multiple germinal sources of dentate granule cells. J Comp Neurol 301**,** 325-342.

Alves-Sampaio, A., Troca-Marin, J. A. and Montesinos, M. L., 2010. NMDA-mediated regulation of DSCAM dendritic local translation is lost in a mouse model of Down's syndrome. J Neurosci 30**,** 13537-13548.

Amaral, D. G., Scharfman, H. E. and Lavenex, P., 2007. The dentate gyrus: fundamental neuroanatomical organization (dentate gyrus for dummies). Prog Brain Res 163**,** 3-22.

Amaral, D. G. and Witter, M. P., 1989. The three-dimensional organization of the hippocampal formation: A review of anatomical data. Neuroscience 31**,** 571-591.

Amaral, D. G. and Witter, M. P., 1995. Hippocampal formation. In: "The Rat Nervous System", G. Paxinos, Academic Press,**,** 443-492.

An, J., Chen, B., Tian, D., Guo, Y., Yan, Y. and Yang, H., 2022. Regulation of Neurogenesis and Neuronal Differentiation by Natural Compounds. Curr Stem Cell Res Ther 17**,** 756-771.

Bahn, S., Mimmack, M., Ryan, M., Caldwell, M. A., Jauniaux, E., Starkey, M., Svendsen, C. N. and Emson, P., 2002. Neuronal target genes of the neuron-restrictive silencer factor in neurospheres derived from fetuses with Down's syndrome: a gene expression study. Lancet 359**,** 310-315.

Bartesaghi, R., Guidi, S. and Ciani, E., 2011. Is it possible to improve neurodevelopmental abnormalities in Down syndrome? Rev Neurosci 22**,** 419-455.

Becker, L. E., Armstrong, D. L., Chan, F. and Wood, M. M., 1984. Dendritic development in human occipital cortical neurons. Brain Res 315**,** 117-124.

Benavides-Piccione, R., Ballesteros-Yanez, I., de Lagran, M. M., Elston, G., Estivill, X., Fillat, C., Defelipe, J. and Dierssen, M., 2004. On dendrites in Down syndrome and DS murine models: a spiny way to learn. Prog Neurobiol 74**,** 111-126.

Bianchi, P., Ciani, E., Guidi, S., Trazzi, S., Felice, D., Grossi, G., Fernandez, M., Giuliani, A., Calza, L. and Bartesaghi, R., 2010. Early pharmacotherapy restores neurogenesis and cognitive performance in the Ts65Dn mouse model for Down syndrome. J Neurosci 30**,** 8769-8779.

Brazel, C. Y., Romanko, M. J., Rothstein, R. P. and Levison, S. W., 2003. Roles of the mammalian subventricular zone in brain development. Prog Neurobiol 69**,** 49-69.

Bull, M. J., 2020. Down Syndrome. N Engl J Med 382**,** 2344-2352.

Cervigni, M., Nasta, L., Schievano, C., Lampropoulou, N. and Ostardo, E., 2019. Micronized Palmitoylethanolamide-Polydatin Reduces the Painful Symptomatology in Patients with Interstitial Cystitis/Bladder Pain Syndrome. Biomed Res Int 2019**,** 9828397.

Chen, P., Liu, Z., Zhang, Q., Lin, D., Song, L., Liu, J., Jiao, H. F., Lai, X., Zou, S., Wang, S., Zhou, T., Li, B. M., Zhu, L., Pan, B. X. and Fei, E., 2022. DSCAM Deficiency Leads to Premature Spine Maturation and Autism-like Behaviors. J Neurosci 42**,** 532-551.

Chen, S., Wang, F., Liu, Z., Zhao, Y., Jiang, Y., Chen, L., Li, C. and Zhou, X., 2019. Brain-derived neurotrophic factor promotes proliferation and progesterone synthesis in bovine granulosa cells. J Cell Physiol 234**,** 8776-8787.

Chen, Y., Niu, J., Li, L., Li, Z., Jiang, J., Zhu, M., Dong, T., Zhang, J., Shi, C., Xu, P., Lu, Y., Jiang, Y., Liu, P. and Chen, W., 2020. Polydatin executes anticancer effects against glioblastoma multiforme by inhibiting the EGFR-AKT/ERK1/2/STAT3-SOX2/Snail signaling pathway. Life Sci 258**,** 118158.

Cherian, S., Hacisayidli, K. M., Kurian, R. and Mathews, A., 2023. Therapeutically important bioactive compounds of the genus Polygonum L. and their possible interventions in clinical medicine. Journal of Pharmacy and Pharmacology 75**,** 301-327.

Costa, A. C. and Scott-McKean, J. J., 2013. Prospects for improving brain function in individuals with down syndrome. CNS Drugs 27**,** 679-702.

Cremon, C., Stanghellini, V., Barbaro, M. R., Cogliandro, R. F., Bellacosa, L., Santos, J., Vicario, M., Pigrau, M., Alonso Cotoner, C., Lobo, B., Azpiroz, F., Bruley des Varannes, S., Neunlist, M., DeFilippis, D., Iuvone, T., Petrosino, S., Di Marzo, V. and Barbara, G., 2017. Randomised clinical trial: the analgesic properties of dietary supplementation with palmitoylethanolamide and polydatin in irritable bowel syndrome. Aliment Pharmacol Ther 45**,** 909-922.

de Graaf, G., Buckley, F. and Skotko, B. G., 2021. Estimation of the number of people with Down syndrome in Europe. Eur J Hum Genet 29**,** 402-410.

Delabar, J. M., Aflalo-Rattenbac, R. and Creau, N., 2006. Developmental defects in trisomy 21 and mouse models. ScientificWorldJournal 6**,** 1945-1964.

Di Nardo, G., Bernardo, L., Cremon, C., Barbara, G., Felici, E., Evangelisti, M., Ferretti, A., Furio, S., Piccirillo, M., Coluzzi, F., Parisi, P., Mauro, A., Di Mari, C., D'Angelo, F. and Mennini, M., 2024.

Palmitoylethanolamide and polydatin in pediatric irritable bowel syndrome: A multicentric randomized controlled trial. Nutrition 122**,** 112397.

Dierssen, M., 2012. Down syndrome: the brain in trisomic mode. Nat Rev Neurosci 13**,** 844-858.

Du, Q. H., Peng, C. and Zhang, H., 2013. Polydatin: a review of pharmacology and pharmacokinetics. Pharm Biol 51**,** 1347-1354.

Ferrer, I. and Gullotta, F., 1990. Down's syndrome and Alzheimer's disease: dendritic spine counts in the hippocampus. Acta Neuropathol 79**,** 680-685.

Fuerst, P. G., Koizumi, A., Masland, R. H. and Burgess, R. W., 2008. Neurite arborization and mosaic spacing in the mouse retina require DSCAM. Nature 451**,** 470-474.

Gardiner, K. J., 2015. Pharmacological approaches to improving cognitive function in Down syndrome: current status and considerations. Drug Des Devel Ther 9**,** 103-125.

Giacomini, A., Stagni, F., Trazzi, S., Guidi, S., Emili, M., Brigham, E., Ciani, E. and Bartesaghi, R., 2015. Inhibition of APP gamma-secretase restores Sonic Hedgehog signaling and neurogenesis in the Ts65Dn mouse model of Down syndrome. Neurobiology of disease 82**,** 385-396.

Guidi, S., Stagni, F., Bianchi, P., Ciani, E., Ragazzi, E., Trazzi, S., Grossi, G., Mangano, C., Calza, L. and Bartesaghi, R., 2013. Early pharmacotherapy with fluoxetine rescues dendritic pathology in the Ts65Dn mouse model of Down syndrome. Brain Pathol 23**,** 129-143.

Haydar, T. F. and Reeves, R. H., 2012. Trisomy 21 and early brain development. Trends Neurosci 35**,** 81-91.

Heberden, C., 2016. Modulating adult neurogenesis through dietary interventions. Nutr Res Rev 29**,** 163-171.

Hsieh, C. P., Chang, W. T., Chen, L., Chen, H. H. and Chan, M. H., 2021. Differential inhibitory effects of resveratrol on excitotoxicity and synaptic plasticity: involvement of NMDA receptor subtypes. Nutr Neurosci 24**,** 443-458.

Huang, B., Liu, J., Meng, T., Li, Y., He, D., Ran, X., Chen, G., Guo, W., Kan, X., Fu, S., Wang, W. and Liu, D., 2018. Polydatin Prevents Lipopolysaccharide (LPS)-Induced Parkinson's Disease via Regulation of the AKT/GSK3β-Nrf2/NF-κB Signaling Axis. Front Immunol 9**,** 2527.

Karami, A., Fakhri, S., Kooshki, L. and Khan, H., 2022. Polydatin: Pharmacological Mechanisms, Therapeutic Targets, Biological Activities, and Health Benefits. Molecules 27**,** 6474.

Kempermann, G. and Gage, F. H., 2002. Genetic influence on phenotypic differentiation in adult hippocampal neurogenesis. Brain Res Dev Brain Res 134**,** 1-12.

Kim, D., Nguyen, M. D., Dobbin, M. M., Fischer, A., Sananbenesi, F., Rodgers, J. T., Delalle, I., Baur, J. A., Sui, G., Armour, S. M., Puigserver, P., Sinclair, D. A. and Tsai, L. H., 2007. SIRT1 deacetylase protects against neurodegeneration in models for Alzheimer's disease and amyotrophic lateral sclerosis. Embo j 26**,** 3169-3179.

Koester, S. E. and O'Leary, D. D., 1992. Functional classes of cortical projection neurons develop dendritic distinctions by class-specific sculpting of an early common pattern. J Neurosci 12**,** 1382-1393.

Kostović, I., Sedmak, G. and Judaš, M., 2019. Neural histology and neurogenesis of the human fetal and infant brain. Neuroimage 188**,** 743-773.

Kumar, V., Pandey, A., Jahan, S., Shukla, R. K., Kumar, D., Srivastava, A., Singh, S., Rajpurohit, C. S., Yadav, S., Khanna, V. K. and Pant, A. B., 2016. Differential responses of Trans-Resveratrol on proliferation of neural progenitor cells and aged rat hippocampal neurogenesis. Sci Rep 6**,** 28142.

Laviola, G., Macrì, S., Morley-Fletcher, S. and Adriani, W., 2003. Risk-taking behavior in adolescent mice: psychobiological determinants and early epigenetic influence. Neurosci Biobehav Rev 27**,** 19-31.

Lu, D., He, L., Xiang, W., Ai, W.-M., Cao, Y., Wang, X.-S., Pan, A., Luo, X.-G., Li, Z. and Yan, X.-X., 2013. Somal and Dendritic Development of Human CA3 Pyramidal Neurons F rom Midgestation to Middle Childhood: A Quantitative Golgi Study. 296**,** 123-132.

Luo, J., Chen, S., Wang, L., Zhao, X. and Piao, C., 2022. Pharmacological effects of polydatin in the treatment of metabolic diseases: A review. Phytomedicine 102**,** 154161.

Lv, C., Zhang, L., Wang, Q., Liu, W., Wang, C., Jing, X. and Liu, Y., 2006. Determination of piceid in rat plasma and tissues by high-performance liquid chromatographic method with UV detection. Biomed Chromatogr 20**,** 1260-1266.

Malberg, J. E., Eisch, A. J., Nestler, E. J. and Duman, R. S., 2000. Chronic antidepressant treatment increases neurogenesis in adult rat hippocampus. J Neurosci 20**,** 9104-9110.

Marin-Padilla, M., 1976. Pyramidal cell abnormalities in the motor cortex of a child with Down's syndrome. A Golgi study. J Comp Neurol 167**,** 63-81.

Maynard, K. R. and Stein, E., 2012. DSCAM contributes to dendrite arborization and spine formation in the developing cerebral cortex. J Neurosci 32**,** 16637-16650.

Mitsogiannis, M. D., Pancho, A., Aerts, T., Sachse, S. M., Vanlaer, R., Noterdaeme, L., Schmucker, D. and Seuntjens, E., 2020. Subtle Roles of Down Syndrome Cell Adhesion Molecules in Embryonic Forebrain Development and Neuronal Migration. Front Cell Dev Biol 8**,** 624181.

Monserrat Hernandez-Hernandez, E., Serrano-Garcia, C., Antonio Vazquez-Roque, R., Diaz, A., Monroy, E., Rodriguez-Moreno, A., Floran, B. and Flores, G., 2016. Chronic administration of resveratrol prevents morphological changes in prefrontal cortex and hippocampus of aged rats. Synapse 70**,** 206-217.

Ni, Z., Tao, L., Xiaohui, X., Zelin, Z., Jiangang, L., Zhao, S., Weikang, H., Hongchao, X., Qiujing, W. and Xin, L., 2017. Polydatin impairs mitochondria fitness and ameliorates podocyte injury by suppressing Drp1 expression. 232**,** 2776-2787.

Nijjar, R. K. and Murphy, C., 2002. Olfactory impairment increases as a function of age in persons with Down syndrome. Neurobiol Aging 23**,** 65-73.

Nowakowski, R. S., Lewin, S. B. and Miller, M. W., 1989. Bromodeoxyuridine immunohistochemical determination of the lengths of the cell cycle and the DNA-synthetic phase for an anatomically defined population. J Neurocytol 18**,** 311-318.

Olmos-Serrano, J. L., Kang, H. J., Tyler, W. A., Silbereis, J. C., Cheng, F., Zhu, Y., Pletikos, M., Jankovic-Rapan, L., Cramer, N. P., Galdzicki, Z., Goodliffe, J., Peters, A., Sethares, C., Delalle, I., Golden, J. A., Haydar, T. F. and Sestan, N., 2016. Down Syndrome Developmental Brain Transcriptome Reveals Defective Oligodendrocyte Differentiation and Myelination. Neuron 89**,** 1208-1222.

Pace, M. C., Passavanti, M. B., Aurilio, C., Sansone, P., Aurilio, R., S, D. E. M., Lama, S., Federico, A., Ravagnan, G., Caraglia, M. and Stiuso, P., 2015. Polydatin administration improves serum biochemical parameters and oxidative stress markers during chronic alcoholism: a pilot study. In Vivo 29**,** 405-408.

Pan, B., Ren, Y. and Liu, L., 2018. Uncovering the action mechanism of polydatin via network pharmacological target prediction. RSC Adv 8**,** 18851-18858.

Pawlonka, J., Rak, B. and Ambroziak, U., 2021. The regulation of cyclin D promoters - review. Cancer Treat Res Commun 27**,** 100338.

Purpura, D. P., 1975. Normal and aberrant neuronal development in the cerebral cortex of human fetus and young infant. UCLA Forum Med Sci**,** 141-169.

Rakic, P., 2009. Evolution of the neocortex: a perspective from developmental biology. Nat Rev Neurosci 10**,** 724-735.

Reagan-Shaw, S., Nihal, M. and Ahmad, N., 2008. Dose translation from animal to human studies revisited. FASEB journal : official publication of the Federation of American Societies for Experimental Biology 22**,** 659-661.

Reinholdt, L. G., Ding, Y., Gilbert, G. J., Czechanski, A., Solzak, J. P., Roper, R. J., Johnson, M. T., Donahue, L. R., Lutz, C. and Davisson, M. T., 2011. Molecular characterization of the translocation breakpoints in the Down syndrome mouse model Ts65Dn. Mamm Genome 22**,** 685-691.

Rice, D. and Barone, S., 2010. Critical periods of vulnerabiliy for the developing nervpus system: evidence from humans and animal models. Environ Health Perspect 108, Suppl 3**,** 511-533.

Ricordi, C., Pacifici, F., Lanzoni, G., Palamara, A. T., Garaci, E. and Della-Morte, D., 2021. Dietary and Protective Factors to Halt or Mitigate Progression of Autoimmunity, COVID-19 and Its Associated Metabolic Diseases. Int J Mol Sci 22.

Roper, R. J., St John, H. K., Philip, J., Lawler, A. and Reeves, R. H., 2006. Perinatal loss of Ts65Dn Down syndrome mice. Genetics 172**,** 437-443.

Rueda, N., Florez, J., Dierssen, M. and Martinez-Cue, C., 2020. Translational validity and implications of pharmacotherapies in preclinical models of Down syndrome. Prog Brain Res 251**,** 245-268.

Saito, Y., Oka, A., Mizuguchi, M., Motonaga, K., Mori, Y., Becker, L. E., Arima, K., Miyauchi, J. and Takashima, S., 2000. The developmental and aging changes of Down's syndrome cell adhesion molecule expression in normal and Down's syndrome brains. Acta Neuropathol (Berl) 100**,** 654-664.

Schimith, L. E., Machado da Silva, V., Costa-Silva, D. G. D., Seregni Monteiro, L. K., Muccillo-Baisch, A. L., André-Miral, C. and Hort, M. A., 2024. Preclinical toxicological assessment of polydatin in zebrafish model. Drug Chem Toxicol**,** 1-10.

Shayganfard, M., 2020. Molecular and biological functions of resveratrol in psychiatric disorders: a review of recent evidence. Cell Biosci 10**,** 128.

Simmons, A. B., Bloomsburg, S. J., Sukeena, J. M., Miller, C. J., Ortega-Burgos, Y., Borghuis, B. G. and Fuerst, P. G., 2017. DSCAM-mediated control of dendritic and axonal arbor outgrowth enforces tiling and inhibits synaptic plasticity. Proc Natl Acad Sci U S A 114**,** E10224-e10233.

Sloviter, R. and Lømo, T., 2012. Updating the Lamellar Hypothesis of Hippocampal Organization. 6.

Şöhretoğlu, D., Baran, M. Y., Arroo, R. and Kuruüzüm-Uz, A., 2018. Recent advances in chemistry, therapeutic properties and sources of polydatin. Phytochemistry Reviews 17**,** 973-1005.

Spalding, K. L., Bergmann, O., Alkass, K., Bernard, S., Salehpour, M., Huttner, H. B., Bostrom, E., Westerlund, I., Vial, C., Buchholz, B. A., Possnert, G., Mash, D. C., Druid, H. and Frisen, J., 2013. Dynamics of hippocampal neurogenesis in adult humans. Cell 153**,** 1219-1227.

Stagni, F. and Bartesaghi, R., 2022. The Challenging Pathway of Treatment for Neurogenesis Impairment in Down Syndrome: Achievements and Perspectives. Front Cell Neurosci 16**,** 903729.

Stagni, F., Giacomini, A., Emili, M., Guidi, S. and Bartesaghi, R., 2018. Neurogenesis impairment: An early developmental defect in Down syndrome. Free Radic Biol Med 114**,** 15-32.

Stagni, F., Giacomini, A., Emili, M., Trazzi, S., Guidi, S., Sassi, M., Ciani, E., Rimondini, R. and Bartesaghi, R., 2016. Short- and long-term effects of neonatal pharmacotherapy with epigallocatechin-3-gallate on hippocampal development in the Ts65Dn mouse model of Down syndrome. Neuroscience 333**,** 277-301.

Stagni, F., Giacomini, A., Guidi, S., Ciani, E. and Bartesaghi, R., 2015a. Timing of therapies for Down syndrome: the sooner, the better. Frontiers in behavioral neuroscience 9**,** 265.

Stagni, F., Giacomini, A., Guidi, S., Ciani, E., Ragazzi, E., Filonzi, M., De Iasio, R., Rimondini, R. and Bartesaghi, R., 2015b. Long-term effects of neonatal treatment with fluoxetine on cognitive performance in Ts65Dn mice. Neurobiol Dis 74C**,** 204-218.

Stagni, F., Giacomini, A., Guidi, S., Emili, M., Uguagliati, B., Salvalai, M. E., Bortolotto, V., Grilli, M., Rimondini, R. and Bartesaghi, R., 2017. A flavonoid agonist of the TrkB receptor for BDNF improves hippocampal neurogenesis and hippocampus-dependent memory in the Ts65Dn mouse model of DS. Exp Neurol 298**,** 79-96.

Stagni, F., Salvalai, M. E., Giacomini, A., Emili, M., Uguagliati, B., Xia, E., Grilli, M., Bartesaghi, R. and Guidi, S., 2019. Neonatal treatment with cyclosporine A restores neurogenesis and spinogenesis in the Ts65Dn model of Down syndrome. Neurobiol Dis 129**,** 44-55.

Stiles, J. and Jernigan, T. L., 2010. The basics of brain development. Neuropsychol Rev 20**,** 327-348.

Takashima, S., Becker, L. E., Armstrong, D. L. and Chan, F., 1981. Abnormal neuronal development in the visual cortex of the human fetus and infant with down's syndrome. A quantitative and qualitative Golgi study. Brain Res 225**,** 1-21.

Takashima, S., Iida, K., Mito, T. and Arima, M., 1994. Dendritic and histochemical development and ageing in patients with Down's syndrome. J Intellect Disabil Res 38 (Pt 3)**,** 265-273.

Takehana, S., Kubota, Y., Uotsu, N., Yui, K., Iwata, K., Shimazu, Y. and Takeda, M., 2017. The dietary constituent resveratrol suppresses nociceptive neurotransmission via the NMDA receptor. Molecular Pain 13**,** 1744806917697010.

Tang, D., Zhang, Q., Duan, H., Ye, X., Liu, J., Peng, W. and Wu, C., 2022. Polydatin: A Critical Promising Natural Agent for Liver Protection via Antioxidative Stress. Oxid Med Cell Longev 2022**,** 9218738.

Tang, J., Li, Y., Wang, J., Wu, Q. and Yan, H., 2019. Polydatin suppresses the development of lung inflammation and fibrosis by inhibiting activation of the NACHT domain-, leucine-rich repeat-, and pyd-containing protein 3 inflammasome and the nuclear factor-κB pathway after Mycoplasma pneumoniae infection. J Cell Biochem 120**,** 10137-10144.

Tang, X.-Y., Xu, L., Wang, J., Hong, Y., Wang, Y., Zhu, Q., Wang, D., Zhang, X.-Y., Liu, C.-Y., Fang, K.-H., Han, X., Wang, S., Wang, X., Xu, M., Bhattacharyya, A., Guo, X., Lin, M. and Liu, Y., 2021. DSCAM/PAK1 pathway suppression reverses neurogenesis deficits in iPSC-derived cerebral organoids from patients with Down syndrome. The Journal of Clinical Investigation 131**,** e135763.

Tozuka, Y., Fukuda, S., Namba, T., Seki, T. and Hisatsune, T., 2005. GABAergic excitation promotes neuronal differentiation in adult hippocampal progenitor cells. Neuron 47**,** 803-815.

Trazzi, S., Mitrugno, V. M., Valli, E., Fuchs, C., Rizzi, S., Guidi, S., Perini, G., Bartesaghi, R. and Ciani, E., 2011. APP-dependent up-regulation of Ptch1 underlies proliferation impairment of neural precursors in Down syndrome. Hum Mol Genet 20**,** 1560-1573.

Tsai, R. Y., Chou, K. Y., Shen, C. H., Chien, C. C., Tsai, W. Y., Huang, Y. N., Tao, P. L., Lin, Y. S. and Wong, C. S., 2012. Resveratrol regulates N-methyl-D-aspartate receptor expression and suppresses neuroinflammation in morphine-tolerant rats. Anesth Analg 115**,** 944-952.

Valenti, D., de Bari, L., de Rasmo, D., Signorile, A., Henrion-Caude, A., Contestabile, A. and Vacca, R. A., 2016. The polyphenols resveratrol and epigallocatechin-3-gallate restore the severe impairment of mitochondria in hippocampal progenitor cells from a Down syndrome mouse model. Biochim Biophys Acta 1862**,** 1093-1104.

Vann, S. D. and Aggleton, J. P., 2002. Extensive cytotoxic lesions of the rat retrosplenial cortex reveal consistent deficits on tasks that tax allocentric spatial memory. Behav Neurosci 116**,** 85-94.

Walle, T., Hsieh, F., DeLegge, M. H., Oatis, J. E., Jr. and Walle, U. K., 2004. High absorption but very low bioavailability of oral resveratrol in humans. Drug Metab Dispos 32**,** 1377-1382.

Workman, A. D., Charvet, C. J., Clancy, B., Darlington, R. B. and Finlay, B. L., 2013. Modeling transformations of neurodevelopmental sequences across mammalian species. J.Neurosci 33**,** 7368-7383.

Xu, C. Y., Li, S., Chen, L., Hou, F. J. and Zhng, R. L., 2011. [Effect of polydatin on learning and memory and expression of NR2B in the prefrontal cortex of rats with chronic alcoholism]. Zhongguo Ying Yong Sheng Li Xue Za Zhi 27**,** 213-214, 220, 235.

Yamaguchi, M., Seki, T., Imayoshi, I., Tamamaki, N., Hayashi, Y., Tatebayashi, Y. and Hitoshi, S., 2016. Neural stem cells and neuro/gliogenesis in the central nervous system: understanding the structural and functional plasticity of the developing, mature, and diseased brain. J Physiol Sci 66**,** 197-206.

Yan, Y., Li, X., Kover, K., Clements, M. and Ye, P., 2013. CREB participates in the IGF-I-stimulation cyclin D1 transcription. Dev Neurobiol 73**,** 559-570.

Zeng, Z., Chen, Z., Li, T., Zhang, J., Gao, Y., Xu, S., Cai, S. and Zhao, K. S., 2015. Polydatin: a new therapeutic agent against multiorgan dysfunction. J Surg Res 198**,** 192-199.

Zgraggen, E., Boitard, M., Roman, I., Kanemitsu, M., Potter, G., Salmon, P., Vutskits, L., Dayer, A. G. and Kiss, J. Z., 2012. Early postnatal migration and development of layer II pyramidal neurons in the rodent cingulate/retrosplenial cortex. Cereb Cortex 22**,** 144-157.

Zhang, L., Huang, Y., Chen, J. Y., Ding, Y. Q. and Song, N. N., 2015. DSCAM and DSCAML1 regulate the radial migration and callosal projection in developing cerebral cortex. Brain Res 1594**,** 61-70.

Zhang, L. X., Li, C. X., Kakar, M. U., Khan, M. S., Wu, P. F., Amir, R. M., Dai, D. F., Naveed, M., Li, Q. Y., Saeed, M., Shen, J. Q., Rajput, S. A. and Li, J. H., 2021. Resveratrol (RV): A pharmacological review and call for further research. Biomed Pharmacother 143**,** 112164.

Zhang, M., Zhao, Z., Shen, M., Zhang, Y., Duan, J., Guo, Y., Zhang, D., Hu, J., Lin, J., Man, W., Hou, L., Wang, H. and Sun, D., 2017. Polydatin protects cardiomyocytes against myocardial infarction injury by activating Sirt3. Biochim Biophys Acta Mol Basis Dis 1863**,** 1962-1972.

FIGURE LEGENDS

Fig. 1. **Study design.** A: Euploid and Ts65Dn pups received a daily injection of either vehicle (Eu + Vehicle; Ts65Dn + Vehicle) or different doses of polydatin (Eu + Poly; Ts65Dn + Poly) from postnatal (P) day 3 (P3) to P15. On P15 they received one BrdU injection 2h before being killed and the brains were subjected to the analyses indicated in the panels on the right. The variables indicated with an asterisk were analyzed in the same mice used in the pilot experiments that had received a dose of 2.5 mg/kg of Poly. B: Euploid and Ts65Dn mice received a daily injection of either vehicle (Eu + Vehicle; Ts65Dn + Vehicle) or 2.5 mg/kg of polydatin (Eu + Poly; Ts65Dn + Poly) starting from P3 until P48-P52 (P50 mice). At this age mice were subjected to a behavioral test (panel on the right). Treatment was continued during behavioral testing. Abbreviations: BrdU, Bromodeoxyuridine; DG, dentate gyrus; Eu, euploid; P, postnatal; PA, Passive Avoidance; Poly, Polydatin. RSC, restrosplenial cortex; SVZ, subventricular zone.

Fig. 2. Effect of neonatal treatment with polydatin on proliferating NPCs in the dentate gyrus of P15 Ts65Dn and euploid mice. A: Representative images of sections immunostained for BrdU from the DG of an euploid and a Ts65Dn mouse treated with vehicle and an euploid and a Ts65Dn mouse treated with 2.5 mg/kg Poly from P3 to P15. Calibration bar=200 μm. B,C: Total number of BrdU-positive cells (B) and mean number of BrdU-positive cells per brain section (C) in the DG of Ts65Dn mice that were treated with vehicle (n=6), 10 mg/kg (n=6), 5 mg/kg (n=3), 2.5 mg/kg (n=4), 1.25 mg/kg (n=3), and 0.625 mg/kg (n=3) of Poly in the period P3-P15. D,E: Total number of BrdU-positive cells (D) and mean number of BrdU-positive cells per brain section (E) in the DG of euploid mice that were treated with vehicle (n=5), 10 mg/kg (n=3), 5 mg/kg (n=3), 2.5 mg/kg (n=3), 1.25 mg/kg (n=3), and 0.625 mg/kg (n=3) of Poly from P3 to P15. F,G: Total number of BrdU-positive cells (F) and mean number of BrdU-positive cells per brain section (G) in the DG of euploid and Ts65Dn mice that were treated with vehicle and Ts65Dn mice that were treated with 10 mg/kg, 5.0 mg/kg, 2.5 mg/kg, 1.25 mg/kg , and 0.625 mg/kg of Poly in the period P3-P15. Same mice as in (B-E). H: Representative images of sections immunostained for Ki-67 from the DG of an euploid and a Ts65Dn mouse treated with vehicle and an euploid and a Ts65Dn mouse

treated with 2.5 mg/kg Poly from P3 to P15. Calibration bar=25 μm- I: Total number of Ki-67-positive cells in the DG of vehicle-treated euploid (n=4) and Ts65Dn (n=4) mice, and euploid (n=4) and Ts65Dn mice (n=4) treated with 2.5 mg/kg of Poly. The scatterplots over each column in (B-G and I) represent the values of individual cases for each group. The asterisks in (B,C) indicate a significant difference in comparison with untreated Ts65Dn mice and the asterisks in (D,F) indicate a significant difference in comparison with untreated euploid mice.. Values in (B-G and I) represent mean ± SE. Values in B, D, F, and I refer to one hemisphere. * $p \leq 0.05$, ** $p \leq 0.01$; *** $p \leq 0.001$ (Fisher's LSD test after one-way or two-way ANOVA; Mann-Whitney test after Kruskal-Wallis test). Abbreviation: d, dorsal; Eu, euploid; GR, granule cell layer; H, hilus; l, lateral; m, medial; MOL, molecular layer; Poly, polydatin; Ts, Ts65Dn; v, ventral; Veh, vehicle.

Fig. 3. Effect of neonatal treatment with polydatin on the size of the population of cells in the S-phase of the cell cycle in the subventricular zone of P15 Ts65Dn and euploid mice. A: Representative image of a section immunostained for BrdU from the subentricular zone overlying the hippocampus. The arrowheads indicate the medial and lateral borders of the SVZ. The star indicates the region of the SVZ within which the examples shown in (B) were taken. Calibration bar=250 μm. B: High magnification images of BrdU-positive cells from the SVZ of an euploid and a Ts65Dn mouse treated with vehicle and an euploid and a Ts65Dn mouse treated with 2.5 mg/kg of Poly from P3 to P15. Calibration bar=50 μm. C,D: Total number of BrdU-positive cells (C) and mean number of BrdU-positive cells per brain section (D) in the SVZ of vehicle-treated euploid (n=5) and Ts65Dn (n=6) mice, and euploid (n=3) and Ts65Dn mice (n=4) treated with 2.5 mg/kg of Poly. Values (mean ± SE) refer to one hemisphere. The scatterplots over each column represent the values of individual cases for each group. * $p \leq 0.05$, ** $p \leq 0.01$; *** $p \leq 0.001$ (Fisher's LSD test after two-way ANOVA). Abbreviation: CA1, CA3, hippocampal fields; d, dorsal; DG, dentate gyrus; Eu, euploid; FH, fissure hippocampica; FI, fimbria; l, lateral; m, medial; Poly, polydatin; SVZ, subventricular zone; TH, thalamus; Ts, Ts65Dn; v, ventral; Veh, vehicle; WM, white matter.

Fig. 4. Effect of neonatal treatment with polydatin on the size of the population of cells in the S-phase of the cell cycle in the retrosplenial cortex of P15 Ts65Dn and euploid mice. A,B: Nissl-stained coronal brain sections

across the rostral border of the RSC (A) and at a caudal distance of approximately 1260 μm (B). The dotted area in (A,B) indicates the region of the RSC where BrdU-positive cells were counted. Calibration bar=500 μm. C: Representative images of sections immunostained for BrdU from the RSC of an euploid and a Ts65Dn mouse treated with vehicle and an euploid and a Ts65Dn mouse treated with 2.5 mg/kg of Poly from P3 to P15. Calibration bar=150 μm. D: Total number of BrdU-positive cells in the RSC of vehicle-treated euploid (n=5) and Ts65Dn (n=6) mice, and euploid (n=3) and Ts65Dn mice (n=4) treated with 2.5 mg/kg of Poly. Values (mean ± SE) refer to one hemisphere. The scatterplots over each column represent the values of individual cases for each group. * $p \leq 0.05$, *** $p \leq 0.001$ (Fisher's LSD test after two-way ANOVA). Abbreviation: CA1, CA3, hippocampal fields; d, dorsal; DG, dentate gyrus; Eu, euploid; FI, fimbria; l, lateral; LV, lateral ventricle; m, medial; Poly, polydatin; RSC, retrosplenial cortex; SVZ, subventricular zone; Ts, Ts65Dn; v, ventral; Veh, vehicle.

Fig. 5. Effect of neonatal treatment with polydatin on granule cell number in the dentate gyrus of P15 Ts65Dn and euploid mice. A: Representative images of DAPI-stained sections showing the DG of an animal from each experimental group. Calibration bar=500 μm. B-D: Volume of the granule cell layer of the DG (B), granule cell density (C), and total number of granule cells (D) of vehicle-treated euploid (n=5) and Ts65Dn (n=6) mice, and euploid (n=3) and Ts65Dn mice (n=4) treated with 2.5 mg/kg of Poly from P3 to P15. Values (mean ± SE) refer to one DG. The scatterplots over each column represent the values of individual cases for each group. * $p \leq 0.05$ (Fisher's LSD test after two-way ANOVA). Abbreviation: d, dorsal; DG, dentate gyrus; Eu, euploid; GR, granule cell layer; H, hilus; l, lateral; m, medial; MOL, molecular layer; Poly, polydatin; Ts, Ts65Dn; v, ventral; Veh, vehicle.

Fig. 6. Effect of neonatal treatment with Poly on dendritic spine density in the dentate gyrus of P15 Ts65Dn and euploid mice. A: Photomicrographs of Golgi-stained granule cell dendrites showing spines on distal dendritic branches in a mouse of each experimental group. Calibration bar=10 μm. B, C: Spine density (mean ± SE) on the proximal (B) and distal (C) dendritic branches of the granule cells of vehicle-treated euploid (n=6) and Ts65Dn (n=5) mice, and euploid (n=5) and Ts65Dn mice (n=4) treated with 2.5 mg/kg of Poly from P3 to P15. Values in

(B, C) represent mean ± SE. The scatterplots over each column represent the values of individual cases for each group. * $p \leq 0.05$; ** $p \leq 0.01$ (Mann-Whitney test after Kruskal-Wallis test). Abbreviations: Eu, euploid; Poly, polydatin; Ts, Ts65Dn; Veh, vehicle.

Fig. 7. Effect of neonatal treatment with Poly on the dendritic architecture of P15 Ts65Dn and euploid mice. A-D: Total dendritic length (A), total number of dendritic branches (B), number (C) and mean length (D) of branches of the different orders of vehicle treated euploid (n=6) and Ts65Dn (n=5) mice and of euploid (n=5) and Ts65Dn (n=4) mice treated with 2.5 mg/kg Poly from P3 to P15. The lack of branches of order 6 in untreated Ts65Dn mice is indicated by a black arrow. E: Dendrograms of the granule cells reconstructed based on the mean length and mean number of branches of each order reported in (C,D). Numbers indicate the branch order starting from the cell body. The number of branches of each order was approximated to the nearest integer value (thick lines). Dashed lines have been used to indicate the number of branches ranging from 0.1 to 0.5. Calibration bar=50 μm. Values in A-D represent mean ± SE. The scatterplots over each column represent the values of individual cases for each group. * $p \leq 0.05$; ** $p \leq 0.01$; *** $p \leq 0.001$ (Fisher's LSD test after two-way ANOVA). Abbreviations: Eu, euploid; Poly, polydatin; Ts, Ts65Dn; Veh, vehicle.

Fig. 8. Effect of neonatal treatment with Poly on the hippocampal levels of Cyclin D1 and DSCAM of P15 Ts65Dn and euploid mice. A: Western blot analysis of Cyclin D1 in hippocampal homogenates of vehicle treated euploid (n=11) and Ts65Dn (n=11) mice and of euploid (n=10) and Ts65Dn (n=9) mice treated with 2.5 mg/kg Poly from P3 to P15. Representative blots are on the left and cumulative data are on the right. B: Immunohistochemical analysis of Cyclin D1 levels in individual NPCs of the SGZ of the dentate gyrus. Representative image of immunostained sections from an euploid and a Ts65Dn mouse treated with vehicle and an euploid and a Ts65Dn mouse treated with 2.5 mg/kg of Poly from P3 to P15 are on the left; cumulative data of vehicle treated euploid (n=4) and Ts65Dn (n=4) mice and of euploid (n=4) and Ts65Dn (n=4) mice are on the right. Calibration bar=20 μm. C: Western blot analysis of DSCAM in hippocampal homogenates of vehicle treated euploid (n=11) and Ts65Dn (n=10) mice and of euploid (n=8) and Ts65Dn (n=8) mice treated with 2.5 mg/kg Poly from P3 to P15. Representative blots are om the left and cumulative data are on the right. Levels of Cyclin

D1 and DSCAM assessed in western blot analysis were normalized to α-Tubulin levels. Data in (A-C) (mean ± SE) are expressed as fold difference in comparison with untreated euploid mice. The scatterplots over each column represent the values of individual cases for each group. * $p \leq 0.05$; ** $p \leq 0.01$ (Fisher's LSD test after two-way ANOVA; Mann-Whitney test after Kruskal-Wallis test). Based on the statistical analysis, one treated euploid mouse was excluded from cyclin D1 western blot analysis. Abbreviations: α-TUB, α-Tubulin; Eu, euploid; GR, granule cell layer; Poly, polydatin; SGZ, subgranular zone; Ts, Ts65Dn; Veh, vehicle.

Fig. 9. Effects of treatment with Poly on cognitive performance in Ts65Dn and euploid mice. Results of the Passive Avoidance test carried out in vehicle treated euploid (n=14) and Ts65Dn (n=9) mice and in euploid (n=21) and Ts65Dn (n=7) mice treated with 2.5 mg/kg Poly from P3 to P48-52. A,B: Latency time for entering the dark compartment on the first day (A) and on the second day (B). On the first day, mice were conditioned with an electrical foot shock when they entered the dark compartment (conditioning). At 24h after the foot shock, mice were reintroduced into the light–dark box and the time it took mice to enter the dark compartment (light–dark latency) was measured. Values represent mean ± SE. The scatterplots over each column represent the values of individual cases for each group. * $p \leq 0.05$; ** $p \leq 0.01$ (Mann-Whitney test after Kruskal-Wallis test). Based on the statistical analysis, two vehicle-treated Ts65Dn mice were excluded from this analysis. Abbreviations: Eu, euploid; Poly, polydatin; Sec, seconds; Ts, Ts65Dn; Veh, vehicle.

Fig. 10. Effects of treatment with Poly on the body and brain weight of P15 and P50 Ts65Dn and euploid mice

A,B**:** Body (A) and brain (B) weight of Ts65Dn mice that were treated with vehicle (n=22), 10 mg/kg (n=6), 5 mg/kg (n=3), 2.5 mg/kg (n=17), 1.25 mg/kg (n=3), and 0.625 mg/kg (n=3) of Poly in the period P3-P15. C,D: Body (C) and brain (D) weight of euploid mice that were treated with vehicle (n=22), 10 mg/kg (n=3), 5 mg/kg (n=3), 2.5 mg/kg (n=18), 1.25 mg/kg (n=3), and 0.625 mg/kg (n=3) of Poly in the period P3-P15. E,F: Body (E) and brain (F) weight of euploid (n=22) and Ts65Dn (n=22) mice treated with vehicle and euploid (n=18) and Ts65Dn (n=17) mice that were treated with 2.5 mg/kg Poly from P3 to P15. Same mice as in (A-D). Mice in (A-F) were used for BrdU immunohistochemistry, Golgi staining and western blotting. Note that in the case of euploid

mice the weight values refer to mice included in these analyses and not to all euploid mice that entered the study (see Methods). G,H: Body (G) and brain (H) weight of euploid (n=14) and Ts65Dn (n=9) mice treated with vehicle and euploid (n=21) and Ts65Dn (n=7) mice that were treated with 2.5 mg/kg Poly from P3 to P48-52. These mice were used for behavioral testing. The asterisks in (A) indicate a significant difference in comparison with untreated Ts65Dn mice and the asterisks in (C-F) indicate a significant difference in comparison with untreated euploid mice. Values in (A-H) represent mean ± SE. The scatterplots over each column represent the values of individual cases for each group. * $p \leq 0.05$; ** $p \leq 0.01$; *** $p \leq 0.001$ (Fisher's LSD test after one-way or two-way ANOVA; Mann-Whitney test after Kruskal-Wallis test). Abbreviations: Eu, euploid; Poly, polydatin; Ts, Ts65Dn; Veh, vehicle.

TABLES

Table 1.

	Euploid		Ts65Dn	
	M	**F**	**M**	**F**
Vehicle	3	2	3	3
Poly 0.625	2	1	2	1
Poly 1.25	2	1	2	1
Poly 2.5	2	1	3	1
Poly 5.0	2	1	1	2
Poly 10.0	2	1	4	2

Number of male (M) and female (F) mice used in pilot experiments that received either vehicle or different doses (expressed as mg/kg body weight) of polydatin (Poly) from P3 to P15. These mice were killed at P15 and used for assessment of the effect of Poly on neural precursor proliferation with BrdU immunohistochemistry in the DG.

Table 2.

	Golgi Staining				Ki-67 and Cyclin D1 IHC			
	Euploid		Ts65Dn		Euploid		Ts65Dn	
	M	F	M	F	M	F	M	F
Vehicle	3	3	3	2	2	2	2	2
Poly 2.5	3	2	3	1	2	2	3	1

Number of male (M) and female (F) mice that received either vehicle or Poly 2.5 mg/kg body weight from P3 to P15, killed at P15 and used for Golgi staining (right hemisphere) and immunohistochemistry (IHC) for Ki-67 and Cyclin D1 (left hemisphere).

Table 3.

WESTERN BLOTTING

	Euploid		Ts65Dn	
	M	**F**	**M**	**F**
Vehicle	6	5	7	4
Poly 2.5	4	6	5	4

Number of male (M) and female (F) mice that received either vehicle or Poly 2.5 mg/kg body weight from P3 to P15, killed at P15 and used for western blotting. The number of mice analyzed for cyclin D1 and DSCAM levels is reported in the legend of Fig. 8.

Table 4.

	Euploid		Ts65Dn	
	M	**F**	**M**	**F**
Vehicle	8	6	2	7
Poly 2.5	13	8	5	2

Number of male (M) and female (F) mice that received either vehicle or Poly 2.5 mg/kg body weight from P3 to P48-52 (P50 mice) and used for the passive avoidance test.

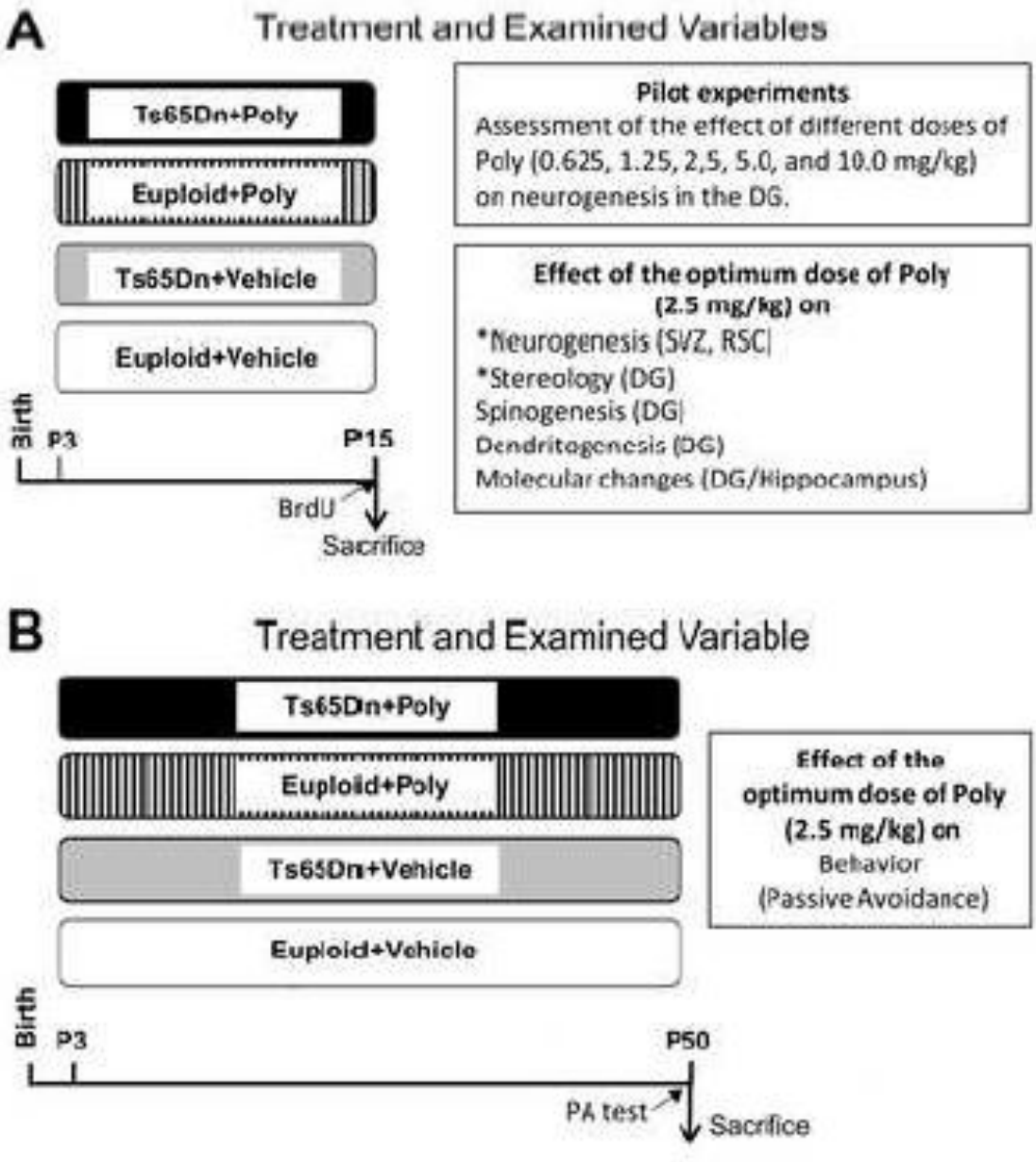
A
Treatment and Examined Variables
Ts65Dn+Poly
Euploid+Poly
Ts65Dn+Vehicle
Euploid+Vehicle
Birth
P3
P15
BrdU
Sacrifice
Pilot experiments
Assessment of the effect of different doses of Poly (0.625, 1.25, 2,5, 5.0, and 10.0 mg/kg) on neurogenesis in the DG.
Effect of the optimum dose of Poly (2.5 mg/kg) on
*Neurogenesis (SVZ, RSC)
*Stereology (DG)
Spinogenesis (DG)
Dendritogenesis (DG)
Molecular changes (DG/Hippocampus)
B
Treatment and Examined Variable
Ts65Dn+Poly
Euploid+Poly
Ts65Dn+Vehicle
Euploid+Vehicle
Birth
P3
P50
PA test
Sacrifice
Effect of the optimum dose of Poly (2.5 mg/kg) on
Behavior
(Passive Avoidance)

Fig. 1

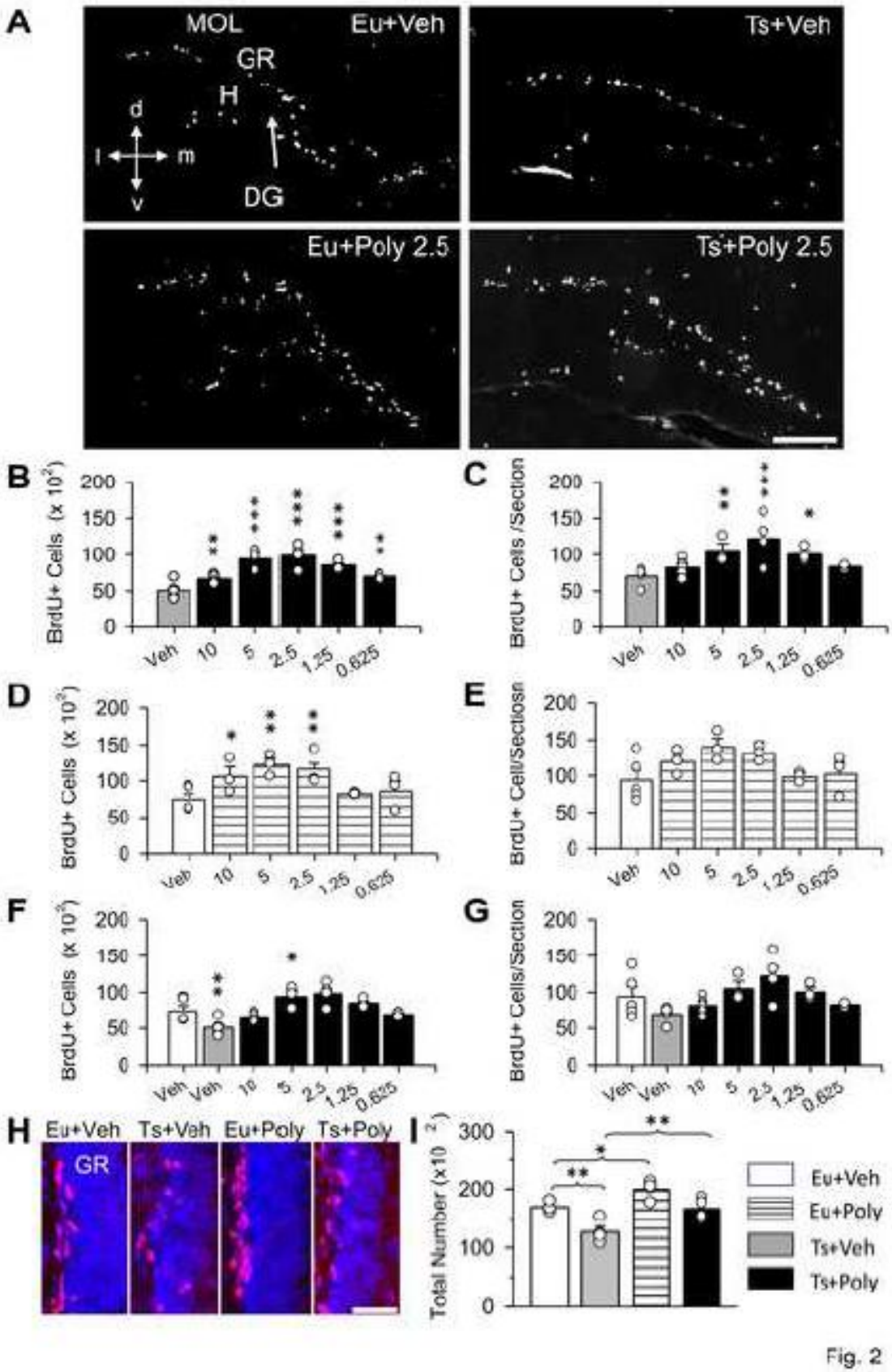
A
MOL
Eu+Veh
GR
H
d
l
m
v
DG
Ts+Veh
Eu+Poly 2.5
Ts+Poly 2.5
B
BrdU+ Cells (x 10²)
C
BrdU+ Cells /Section
D
BrdU+ Cells (x 10²)
E
BrdU+ Cell/Sectiosn
F
BrdU+ Cells (x 10²)
G
BrdU+ Cells/Section
Veh
10
5
2.5
1.25
0.625
H
Eu+Veh
Ts+Veh
Eu+Poly
Ts+Poly
GR
I
Total Number (x10 ²)
Eu+Veh
Eu+Poly
Ts+Veh
Ts+Poly

Fig. 2

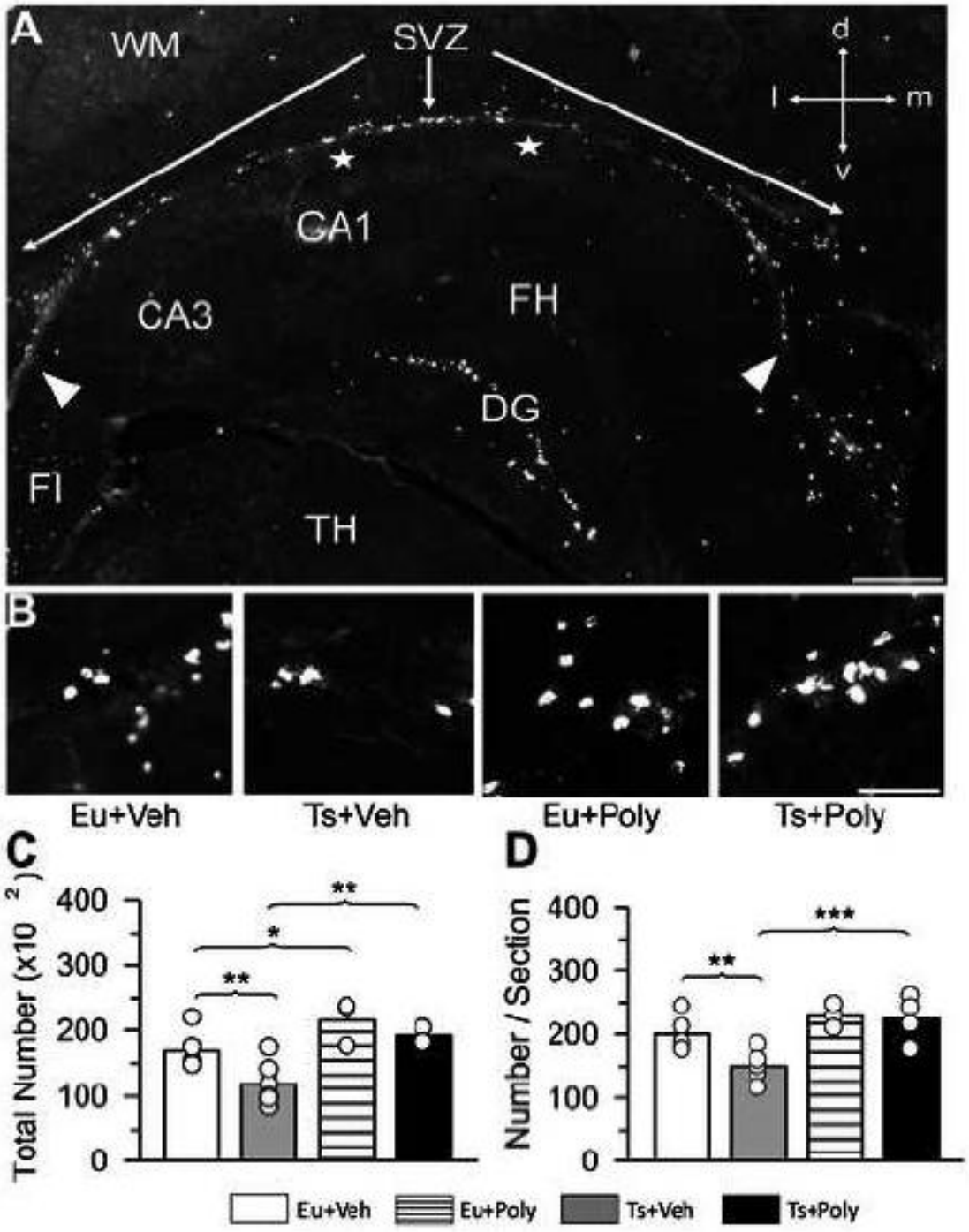
A
WM
SVZ
d
l
m
v
CA1
CA3
FH
DG
Fl
TH
B
Eu+Veh
Ts+Veh
Eu+Poly
Ts+Poly
C
Total Number (x10 2)
400
300
200
100
0
**
*
**
D
Number / Section
400
300
200
100
0
**
***
Eu+Veh
Eu+Poly
Ts+Veh
Ts+Poly

Fig. 3

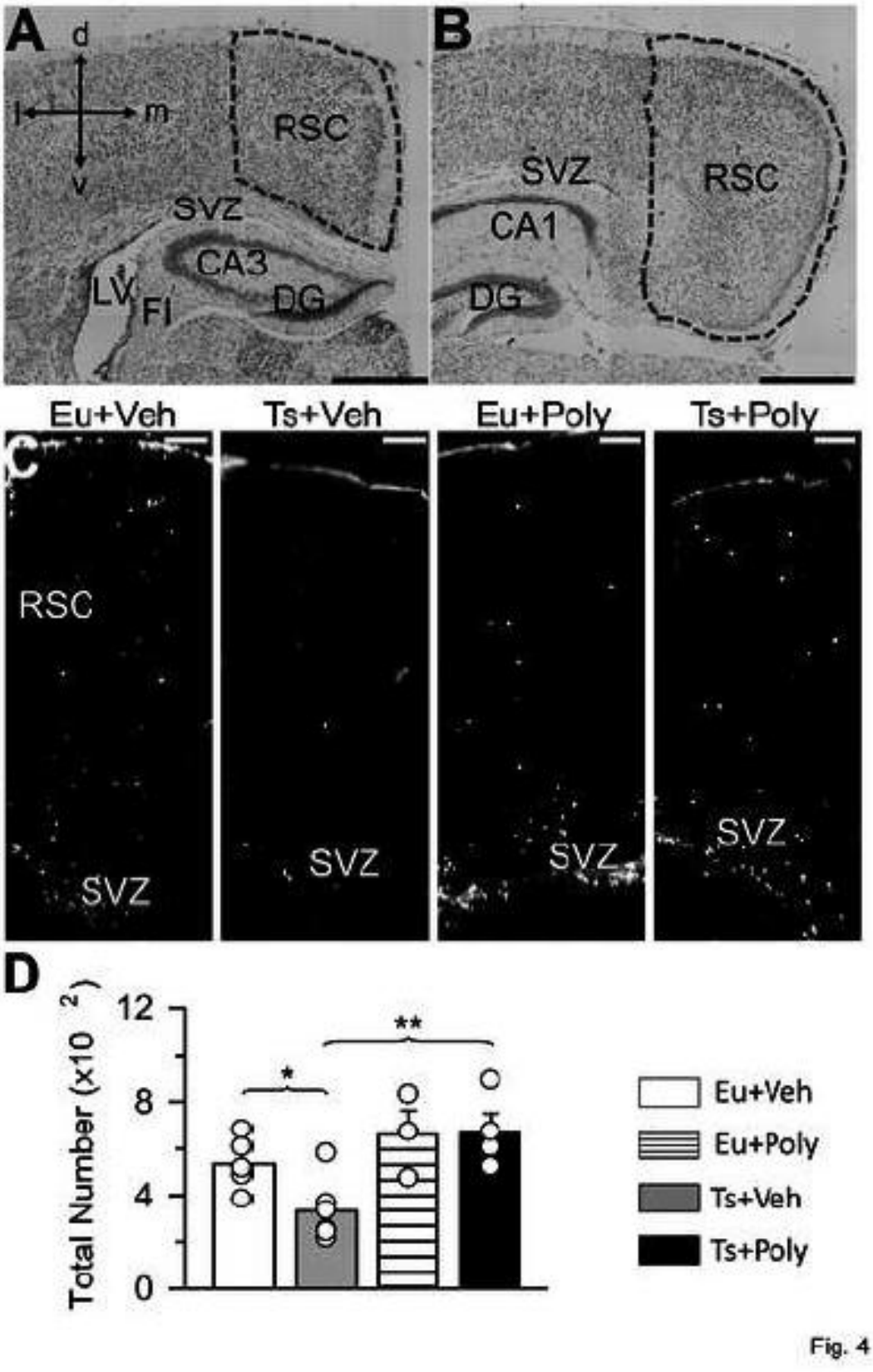
A
d
l
m
v
RSC
SVZ
CA3
LV
FI
DG
B
SVZ
RSC
CA1
DG
Eu+Veh
Ts+Veh
Eu+Poly
Ts+Poly
C
RSC
SVZ
SVZ
SVZ
SVZ
D
Total Number (x10 2)
12
8
4
0
*
**
Eu+Veh
Eu+Poly
Ts+Veh
Ts+Poly

Fig. 4

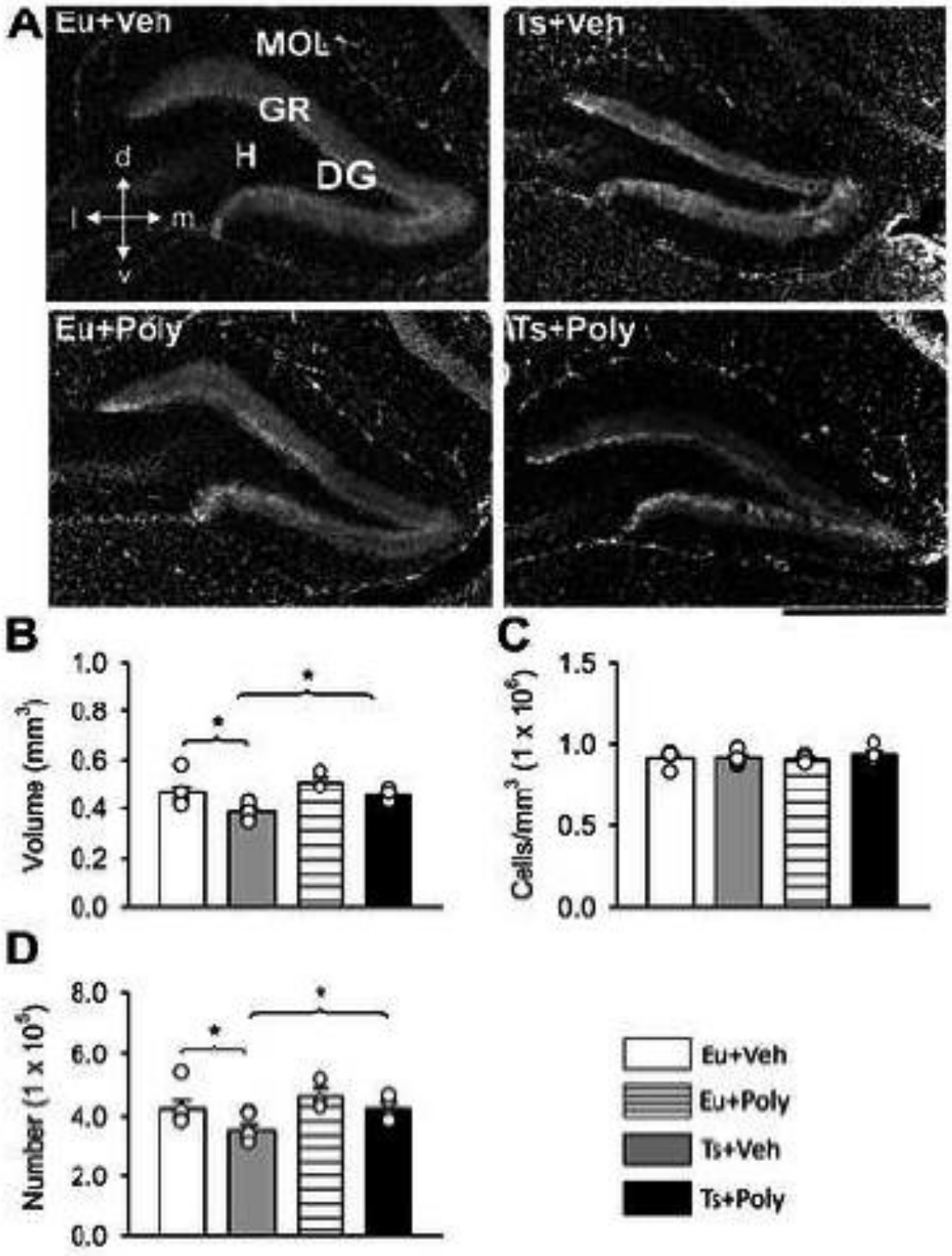
A
Eu+Veh
MOL
GR
H
DG
d
l
m
v
Ts+Veh
Eu+Poly
Ts+Poly
B
Volume (mm3)
1.0
0.8
0.6
0.4
0.2
0.0
C
Cells/mm3 (1 x 10^6)
1.5
1.0
0.5
0.0
D
Number (1 x 10^6)
8.0
6.0
4.0
2.0
0.0
Eu+Veh
Eu+Poly
Ts+Veh
Ts+Poly

Fig. 5

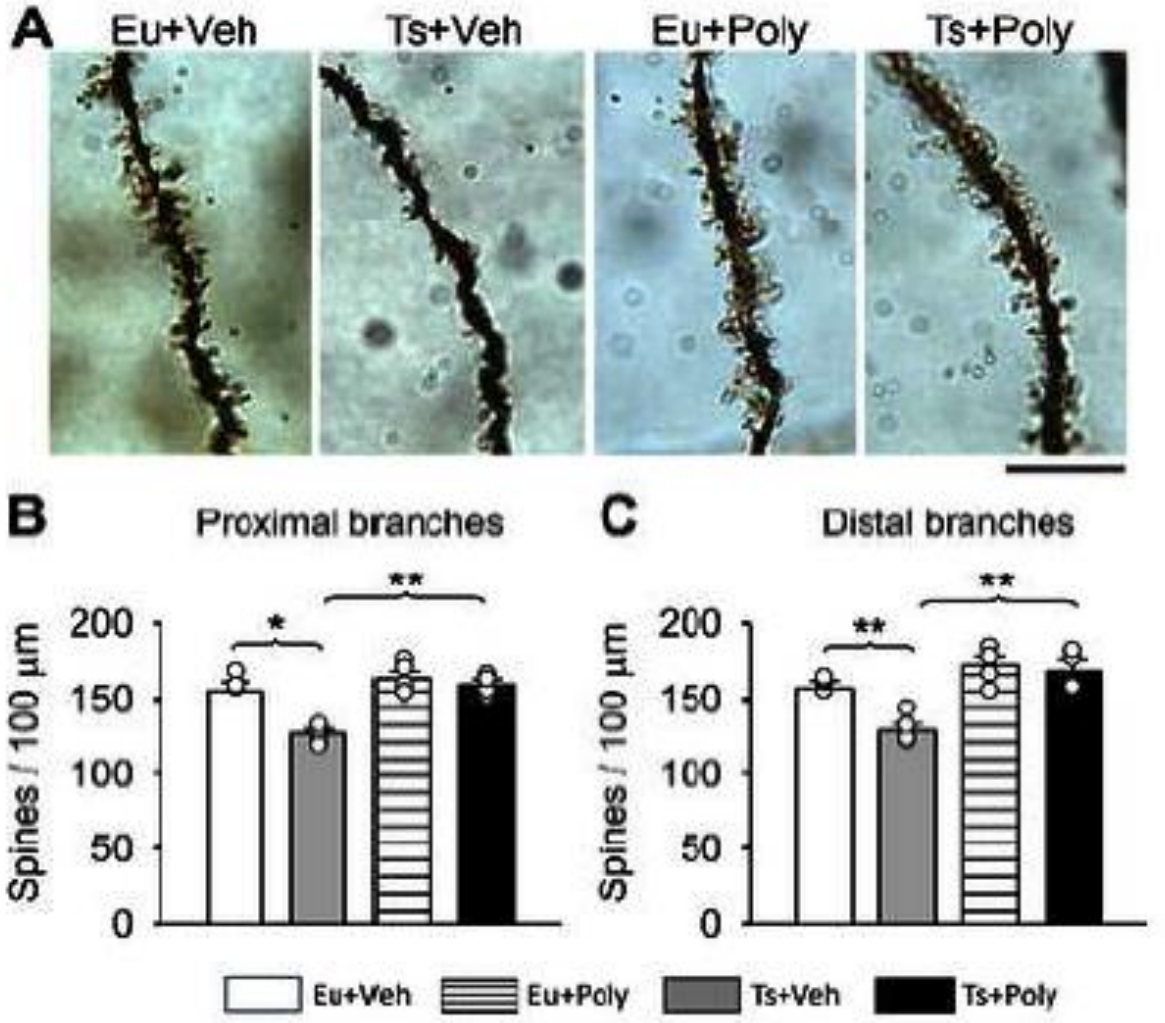
A
Eu+Veh
Ts+Veh
Eu+Poly
Ts+Poly
B
Proximal branches
C
Distal branches
Spines / 100 µm
200
150
100
50
0
*
**
**
Eu+Veh
Eu+Poly
Ts+Veh
Ts+Poly

Fig. 6

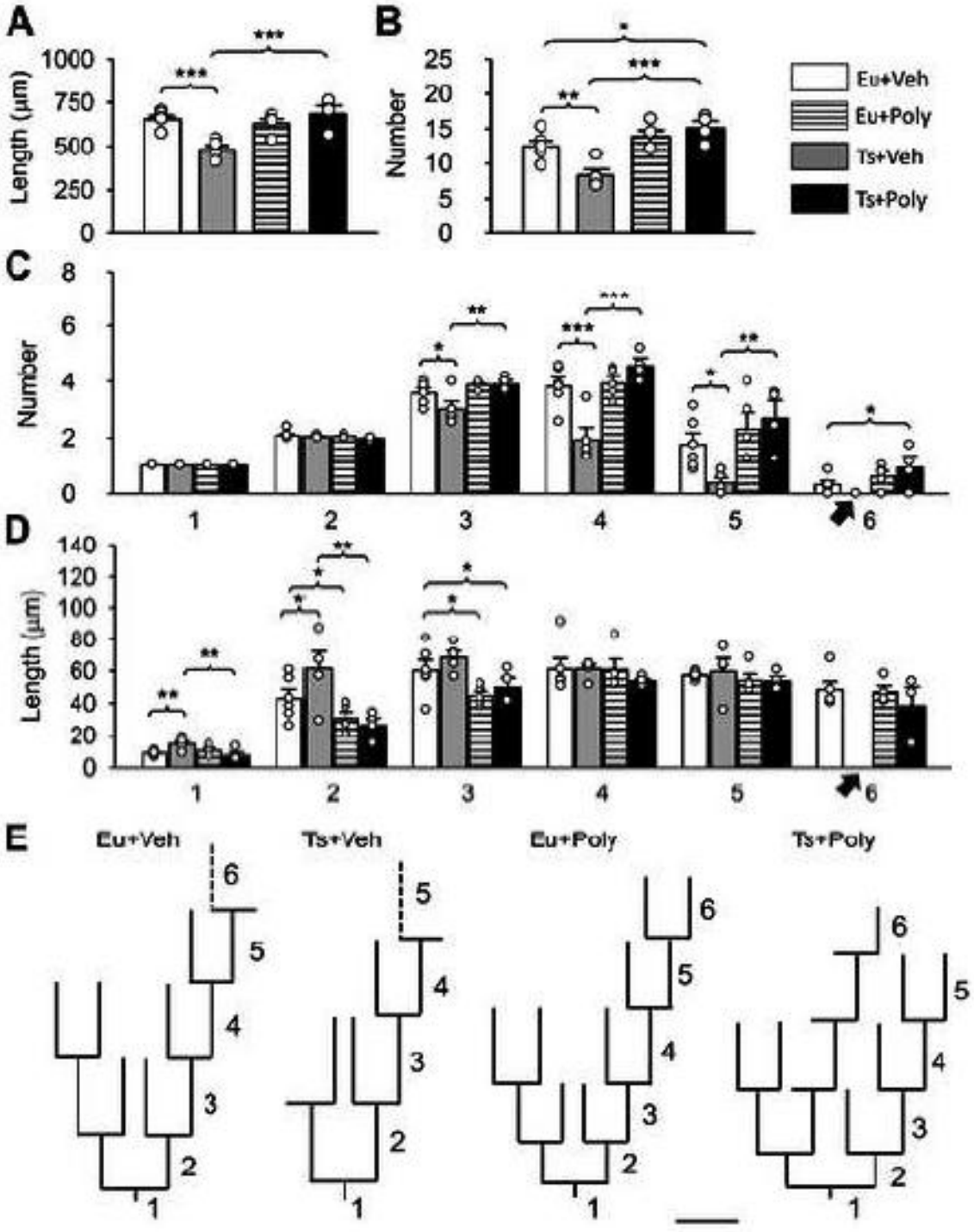
A
Length (µm)
1000
750
500
250
0
***
***
B
Number
25
20
15
10
5
0
*
***
**
Eu+Veh
Eu+Poly
Ts+Veh
Ts+Poly
C
Number
8
6
4
2
0
1
2
3
4
5
6
D
Length (µm)
140
120
100
80
60
40
20
0
E
Eu+Veh
Ts+Veh
Eu+Poly
Ts+Poly

Fig. 7

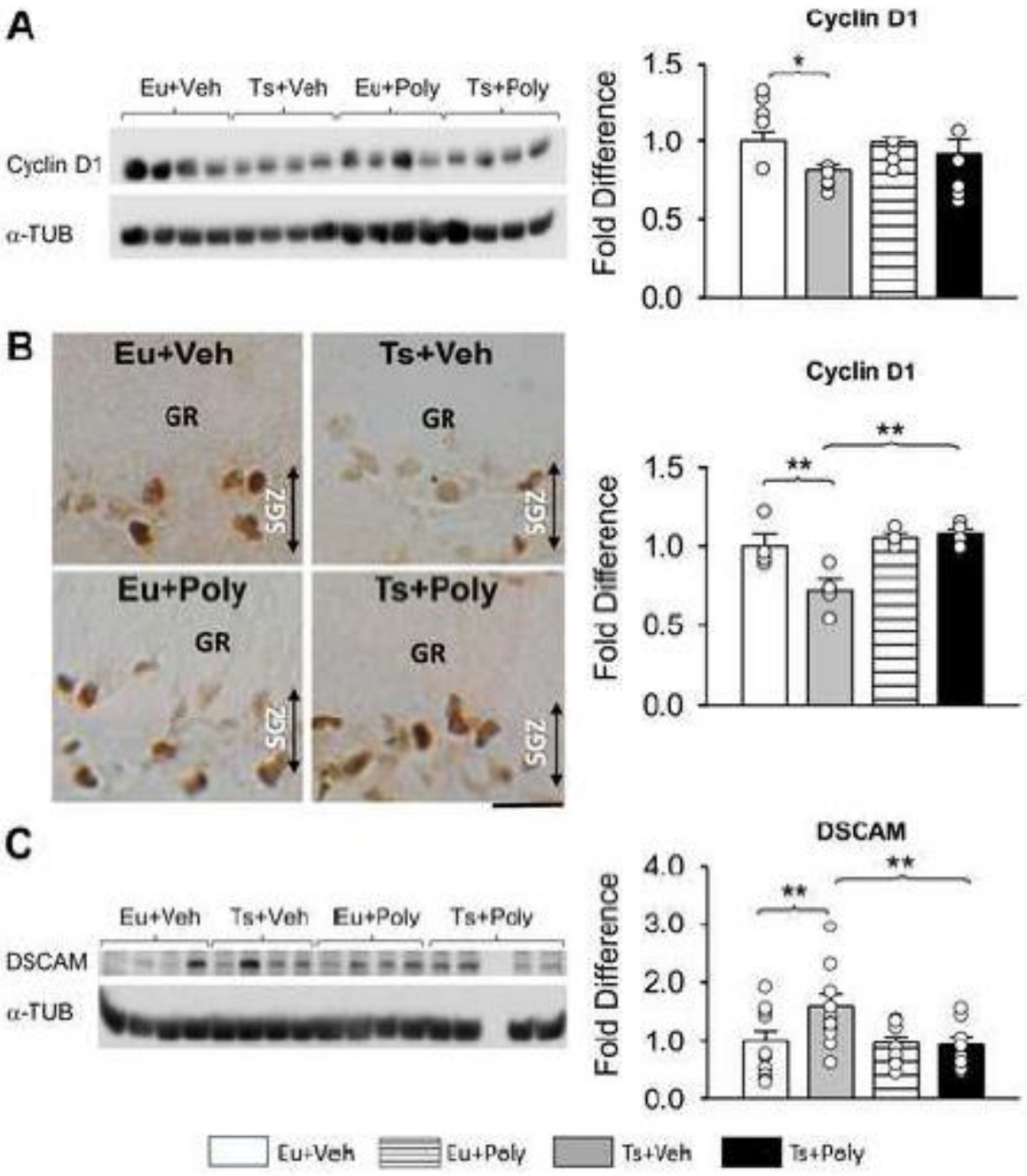
A
Eu+Veh
Ts+Veh
Eu+Poly
Ts+Poly
Cyclin D1
α-TUB
Cyclin D1
Fold Difference
1.5
1.0
0.5
0.0
*
B
Eu+Veh
GR
SGZ
Ts+Veh
GR
SGZ
Eu+Poly
GR
SGZ
Ts+Poly
GR
SGZ
Cyclin D1
Fold Difference
1.5
1.0
0.5
0.0
**
**
C
Eu+Veh
Ts+Veh
Eu+Poly
Ts+Poly
DSCAM
α-TUB
DSCAM
Fold Difference
4.0
3.0
2.0
1.0
0.0
**
**
Eu+Veh
Eu+Poly
Ts+Veh
Ts+Poly

Fig. 8

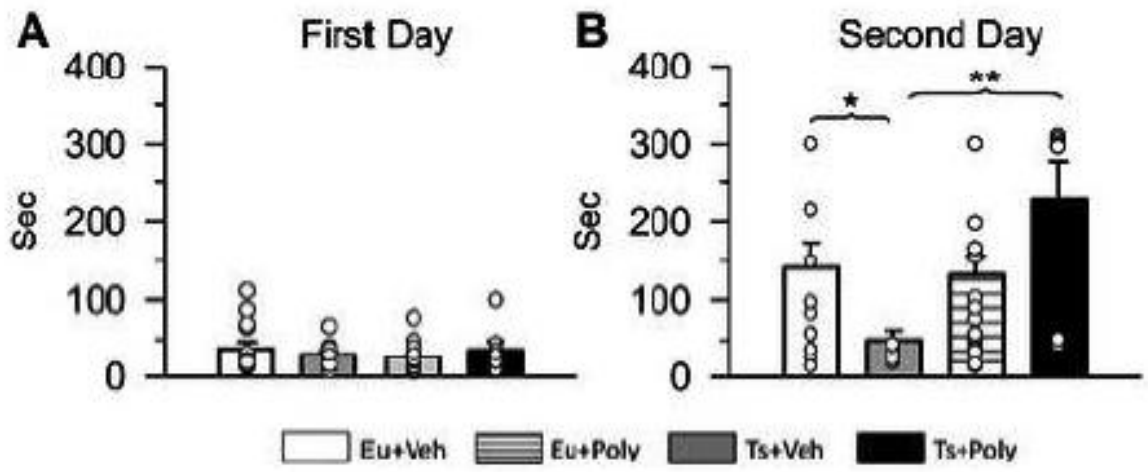
A
First Day
B
Second Day
Sec
400
300
200
100
0
*
**
Eu+Veh
Eu+Poly
Ts+Veh
Ts+Poly

Fig. 9

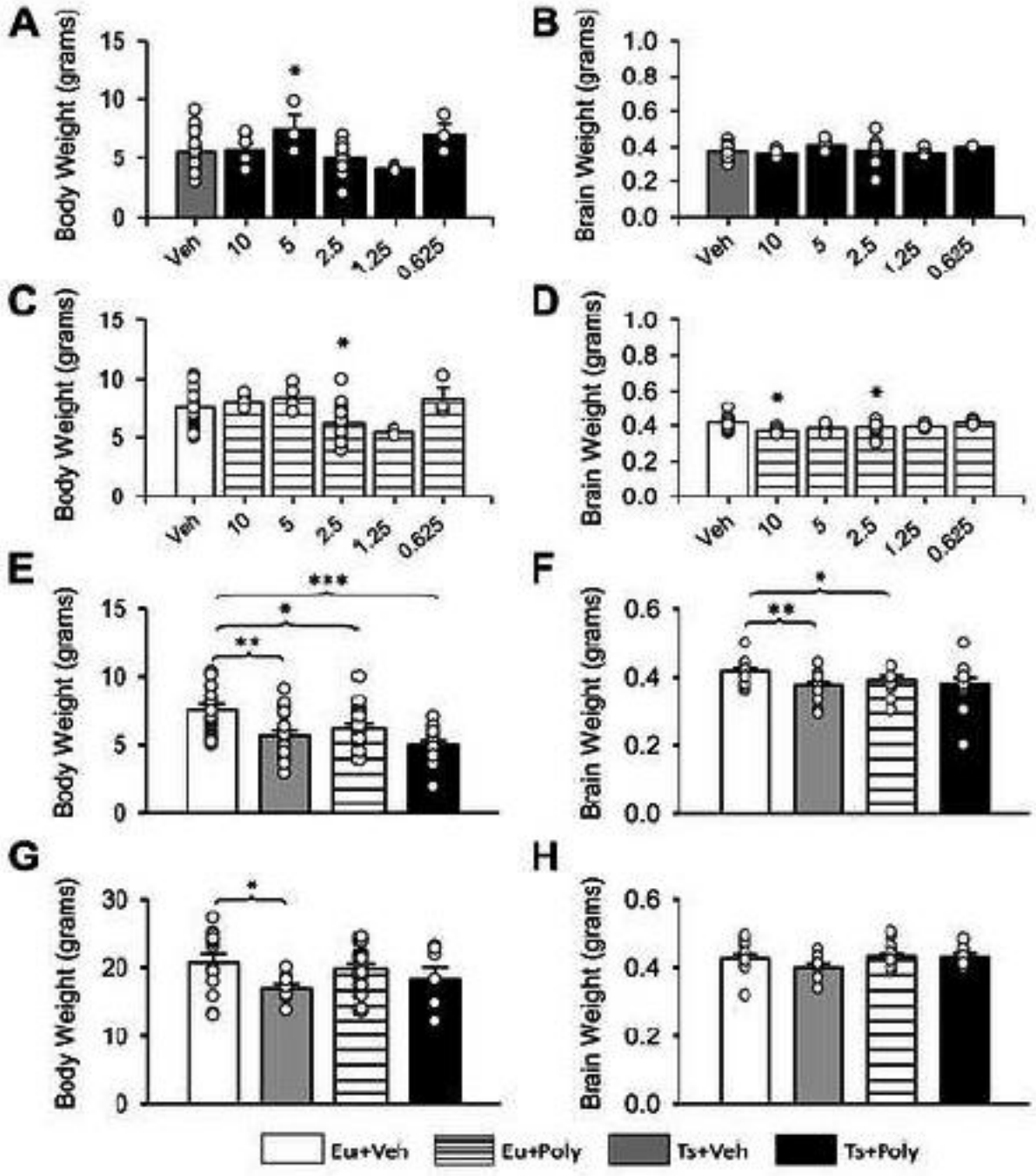
A
Body Weight (grams)
15
10
5
0
Veh
10
5
2.5
1.25
0.625
B
Brain Weight (grams)
1.0
0.8
0.6
0.4
0.2
0.0
C
D
E
F
G
H
***
**
*
30
20
Eu+Veh
Eu+Poly
Ts+Veh
Ts+Poly

Fig. 10